Massive MIMO-Enabled Full-Duplex Cellular Networks

Arman Shojaeifard, *Member, IEEE*, Kai-Kit Wong, *Fellow, IEEE*,
Marco Di Renzo, *Senior Member, IEEE*, Gan Zheng, *Senior Member, IEEE*,
Khairi Ashour Hamdi, *Senior Member, IEEE*, Jie Tang, *Member, IEEE*

arXiv:1611.03854v1 [cs.IT] 11 Nov 2016

Abstract

In this paper, we provide a theoretical framework for the study of massive multiple-input multiple-output (MIMO)-enabled full-duplex (FD) cellular networks in which the self-interference (SI) channels follow the Rician distribution and other channels are Rayleigh distributed. To facilitate bi-directional wireless functionality, we adopt (i) a downlink (DL) linear zero-forcing with self-interference-nulling (ZF-SIN) precoding scheme at the FD base stations (BSs), and (ii) an uplink (UL) self-interference-aware (SIA) fractional power control mechanism at the FD user equipments (UEs). Linear ZF receivers are further utilized for signal detection in the UL. The results indicate that the UL rate bottleneck in the baseline FD single-antenna system can be overcome via exploiting massive MIMO. On the other hand, the findings may be viewed as a reality-check, since we show that, under state-of-the-art system parameters, the spectral efficiency (SE) gain of FD massive MIMO over its half-duplex (HD) counterpart largely depends on the SI cancellation capability of the UEs.

Index Terms

Full-Duplex, Large Scale Antenna Array, Self-Interference, Linear Processing, Power Control, Rician Fading.

I. Introduction

The fifth-generation mobile network (5G) is expected to roll out from 2018 onwards as a remedy for tackling the existing capacity crunch [1]. A key 5G technology is massive multiple-input multiple-output (MIMO), or large scale antenna system (LSAS), where the base stations (BSs) equipped with hundreds of antennas simultaneously communicate with multiple user equipments (UEs) [2]. Massive MIMO, via spatial-multiplexing and directing power intently, can greatly outperform the state-of-the-art cellular standards jointly in terms of spectral efficiency (SE) and energy efficiency (EE) [3], [4]. Moreover, under increasingly scarce spectrum, the transcieving of information over the same radio-frequency (RF) resources, i.e. full-duplex (FD) mode [5], has become a candidate solution for 5G and beyond [6], [7]. In theory, FD mode can achieve double the sum-rate versus that in a half-duplex (HD) system, where orthogonal RF partitioning is typically employed to avoid the over-powering self-interference (SI). In practice, however, the FD over HD SE gain predominantly depends on the SI cancellation capability.

There's been major breakthroughs in SI cancellation using any combination of (i) spatial/angular isolation and (ii) subtraction in digital/analog domains [8]. FD, beyond point-to-point, is however not well understood. In particular, the introduction of cross-mode interference (CI) between the downlink (DL) and the uplink (UL), as well as SI, significantly increases the complexity for FD cellular setups. Many relevant works have emerged recently, including FD for small-cell (SC) [9], [10], relay (RL) [11]–[13], cloud radio access network (CRAN) [14], and heterogeneous cellular network (HCN) [15]–[17]. A general consensus from early results is that the FD over HD SE gain mostly arises in the DL and that the UL is the main performance bottleneck. The authors in [18] have shown that bi-directional cellular systems with single-input single-output (SISO) transmission, achieve double the DL rate at the cost of more than a thousand-fold reduction in the UL rate. A potential strategy for tackling this limitation is to exploit the large degrees of freedom (DoF) in massive MIMO for better resilience against SI and CI [19], [20].

In [21], the authors considered a FD massive MIMO BS with multiple HD SISO UEs, and proposed a linear extended zero-forcing (ZF) precoder to supress SI at the receiving antennas, subject to perfect channel state information (CSI). The sum-rate with FD mode was almost doubled versus that in the HD case, and the optimal ratio of transmit over receive antennas was found to be approximately 3 [21]. The extension to a FD massive MIMO BS serving MIMO HD UEs using linear block diagonalization (BD) beamforming was studied in [22]. With asymptotically large antenna array, the optimal ratio of transmit

A. Shojaeifard and K.-K Wong are with the Communications and Information Systems Research Group, Department of Electronic and Electrical Engineering, University College London, London, United Kingdom (e-mail: a.shojaeifard@ucl.ac.uk; kai-kit.wong@ucl.ac.uk).

M. Di Renzo is with the Laboratoire des Signaux et Systèmes, CNRS, CentraleSupélec, Univ Paris Sud, Université Paris-Saclay, Gif-sur-Yvette, France (e-mail: marco.direnzo@l2s.centralesupelec.fr).

G. Zheng is with the Signal Processing and Networks Research Group, Wolfson School of Mechanical, Electrical and Manufacturing Engineering, Loughborough University, Loughborough, United Kingdom (e-mail: g.zheng@lboro.ac.uk).

K. A. Hamdi is with the Microwave and Communication Systems Research Group, School of Electrical and Electronic Engineering, University of Manchester, Manchester, United Kingdom (e-mail: k.hamdi@manchester.ac.uk).

J. Tang is with the Smart Information Processing Centre, School of Electronic and Information Engineering, South China University of Technology, Guangzhou, China (e-mail: eejtang@scut.edu.cn).

This work was supported by the Engineering and Physical Sciences Research Council (EPSRC) under grant EP/N008219/1.

over receive antennas was shown to converge to the ratio of DL over UL streams. In [23], under a setup similar to that in [21], the FD sum-rate with different spatial isolation and SI subtraction techniques was compared considering both perfect and imperfect CSI. On the other hand, non-linear transceiver design for maximizing the sum-rate in FD multi-user MIMO has been studied in [24] and [25]. The works highlighted considered a single-cell network. Intuitively, the introduction of SI and CI has huge implications in a FD multi-cell multi-user MIMO paradigm necessitating rigorous investigation.

Motivated by the above, a theoretical stochastic geometry-based framework for the study of FD massive MIMO cellular networks using the Poisson point process (PPP)-based abstraction model is presented. We jointly consider the DL and the UL of a multi-cell FD setup where BSs with massive antennas and the UEs are transceiving over the same RF resources. We adopt the Rician distribution for the SI fading channels, thus capturing performance under generalized SI cancellation capability. All other fading channels are modeled using the Rayleigh distribution.

In the DL, we devise a linear zero-forcing with self-interference-nulling (ZF-SIN) precoder to jointly suppress multi-user interference and SI under perfect CSI. On the other hand, the total number of antennas at the UEs is limited due to the physical size of the devices. Hence, we propose a self-interference-aware (SIA) fractional power control mechanism at the FD UEs to keep SI below a certain level. We derive the distributions, and in certain cases higher-order statistics of the transmit power. In the UL, for signal detection at the FD massive MIMO BSs, linear ZF receivers are utilized for suppressing multi-user interference. The signals distributions are derived under the linear processes described above. We characterize the SEs using a moment-generating-function (m.g.f.)-based approach and derive the signals conditional statistics in closed-form. The FD SE expressions provided require a three-fold integration, versus the manifold integrals involved in the direct capacity evaluation approach. We further reduce the complexity in certain cases and derive tight bounded closed-form expressions of the DL and the UL SEs with SISO. Under this setup, we tackle the problem of finding the optimal ratio of BS over UE transmit powers which results in the highest FD over HD sum-rate gain. We prove that the ratio of FD over HD SEs is quasi-convex in the set of positive transmit powers. The corresponding optimal point is found to converge to the ratio of the transmit powers being equal to one.

The validity of the theoretical findings is confirmed using Monte-Carlo (MC) simulations. The results highlight that the key features of massive MIMO, in terms of high transmit/receive array gain and lower BS/UE transmit power, allow for achieving significant performance gains over other FD cellular setups. On the other hand, the SE gain of FD over HD massive MIMO cellular network was shown to be largely dependent on the SI cancellation capability of the UEs.

The massive MIMO-enabled FD setup is described in Section II. The different signals are modeled in Section III. The power control mechanism is introduced in Section IV. The SE analysis is provided in Section V, followed by a comparison of FD over HD in Section VI. Numerical results are provided in Section VII, and finally, conclusions are drawn in Section VIII.

Notation: $\boldsymbol{X}$ is a matrix with (i,j)-th entry $\{\boldsymbol{X}\}_{i,j}$; $\boldsymbol{x}$ is a vector with k-th element $\{\boldsymbol{x}\}_k$; T, $\dagger$, and $+$ are the transpose, Hermitian, and pseudo-inverse operations; $\mathbb{E}_x\{.\}$ is the expectation; $\mathcal{F}_x(.)$ is the cumulative density function (c.d.f.); $\mathcal{P}_x(.)$ is the probability density function (p.d.f.); $\mathscr{P}(x)$ is the probability; $\mathcal{M}_x(.)$ is the m.g.f.; $|x|$ is the modulus; $\|\boldsymbol{x}\|$ and $\|\boldsymbol{X}\|$ are the Euclidean and Frobenius norms; $\mathbf{I}_{(.)}$ is the identity matrix; Null$(.)$ is a nullspace; $\mathcal{H}(.)$ is the Heaviside step function; $\delta(.)$ is the Delta function; $\Gamma(.)$ and $\Gamma(.,.)$ are the Gamma and incomplete (upper) Gamma functions; $\mathcal{L}_n(.)$ is the Laguerre polynomial; Ei$(.)$, $\mathscr{S}(.)$, and $\mathscr{C}(.)$ are the exponential, Sine, and Cosine integral functions; erfi$(.)$ is the imaginary error function; $Q_m(.,.)$ is the Marcum Q-function; ${}_2F_1(.,.;.;.)$, ${}_2\tilde{F}_1(.,.;.;.)$, ${}_0F_1\left(;.;.\right)$, ${}_0\tilde{F}_1\left(;.;.\right)$, ${}_pF_q(.;.;.)$, ${}_p\tilde{F}_q(.;.;.)$ are the Gauss, Regularized Gauss, confluent, Regularized confluent, generalized, and Regularized generalized hypergeometric functions; and $\mathcal{G}_{p,q}^{m,n}\left(\cdot\middle|(.)\right)$ is the Meijer-G function, respectively.

II. Modeling Preliminaries

Consider a FD cellular setup with BSs and UEs respectively deployed on the Euclidean grid according to independent stationary PPPs $\Phi^{(b)}$ and $\Phi^{(u)}$ with spatial densities $\lambda^{(b)}$ and $\lambda^{(u)}$. Let y_l and x_k denote the locations of the l-th BS and the k-th UE, respectively. Their respective Euclidean distance is therefore $d_{y_l,x_k} = \|y_l - x_k\|$. The BSs are assumed to have $N = N_t + N_r$ antennas where N_t and N_r are respectively the number of RF transmit and receive chains. The UEs are in turn assumed to be equipped with a single RF transmit/receive chain (i.e., two antennas in total). In the DL, the BSs simultaneously serve $\mathcal{U}$ UEs per resource block using linear transmit precoding. In the UL, the scheduled UEs simultaneously transmit to their serving massive MIMO BS per resource block [26]. Linear receive filters are then used for UL signal detection. We assume the condition $\mathcal{U} \leq \min(N_t, N_r)$ holds, thus scheduling is not necessary here.

Let $\boldsymbol{g}_{y_l,x_k} \in \mathcal{C}^{1\times N_t}$, $\boldsymbol{G}_{y_l,y_j} \in \mathcal{C}^{N_r\times N_t}$, and $\boldsymbol{G}_{y_l,y_l} \in \mathcal{C}^{N_r\times N_t}$ denote the channel from the l-BS to the k-th UE, the channel from the l-th BS to the j-th BS, and the SI channel at the l-th BS, respectively. Moreover, $\boldsymbol{h}_{x_k,y_l} \in \mathcal{C}^{N_r\times 1}$, h_{x_k,x_i}, and h_{x_k,x_k} are respectively the channel from the k-th UE to the l-th BS, the channel from the k-th UE to the i-th UE, and the SI channel at the k-th UE. The SI channels are subject to Rician fading with independent and identically-distributed (i.i.d.) elements drawn from $\mathcal{CN}(\mu, \upsilon^2)$. All other channels are modeled using Rayleigh fading with i.i.d. elements drawn from $\mathcal{CN}(0,1)$. We use the unbounded distance-dependent path-loss model with exponent β (> 2). Perfect CSI is assumed to be available through UL training [27].

By invoking the Campbell's theorem, the DL analysis is on an arbitrary UE k^* assumed to be located at the center. We consider a cellular association strategy where the UE k^* is exclusively served by a BS l^* which provides the greatest received

signal power. For homogeneous deployments, this is equivalent to the cell selection approach based on the closest distance [28]

$$y_{l^*} = \arg\max \left(\left\| d_{y_l, x_{k^*}} \right\|^{-\beta} \right), \ \forall y_l \in \Phi^{(b)}. \tag{1}$$

The UL analysis, on the other hand, is carried out for the reference UE at its serving BS. Similarly, all other scheduled UEs in the system are assumed to have been exclusively associated with their closest deployed BS. With a slight abuse of notation, let x_k^l denote the location of the k-th scheduled UE of the BS located at y_l. For consistency's sake, $x_{k^*}^{l^*}$ is thus used in place of x_{k^*} where the context is clear. The reference transceiver distance p.d.f. can be expressed as

$$\mathcal{P}_{d_{y_{l^*}, x_{k^*}^{l^*}}}(r) = 2\pi\lambda^{(b)} r \exp\left(-\pi\lambda^{(b)} r^2\right). \tag{2}$$

It is important to highlight that the alternative decoupling approach for cellular association [29] results in the loss of channel reciprocity in massive MIMO systems.

III. Signals Definitions

Let $\boldsymbol{G}_{y_l} = [\boldsymbol{g}_{y_l, x_k^l}^T]_{1 \le k \le \mathcal{U}}^T \in \mathcal{C}^{\mathcal{U} \times N_t}$ denote the combined DL channels from the l-th BS to its $\mathcal{U}$ UEs. We use $\boldsymbol{s}_{y_l} = [s_{y_l, x_k^l}]_{1 \le k \le \mathcal{U}}^T \in \mathcal{C}^{\mathcal{U} \times 1}$, $\mathbb{E}\{|s_{y_l, x_k^l}|^2\} = 1$, to denote the DL complex symbol vector from the l-th BS to its $\mathcal{U}$ UEs. The transmit signal vector with linear precoding at the l-th BS is $\boldsymbol{t}_{y_l} = \boldsymbol{V}_{y_l} \boldsymbol{s}_{y_l}$ where $\boldsymbol{V}_{y_l} = [\boldsymbol{v}_{y_l, x_k^l}]_{1 \le k \le \mathcal{U}} \in \mathcal{C}^{N_t \times \mathcal{U}}$ is the precoding matrix. The DL received signal is

$$\begin{aligned} y_d = & \underbrace{\sqrt{\frac{p^{(b)}}{\mathcal{U}}} d_{y_{l^*}, x_{k^*}^{l^*}}^{-\frac{\beta}{2}} \boldsymbol{g}_{y_{l^*}, x_{k^*}^{l^*}} \boldsymbol{v}_{y_{l^*}, x_{k^*}^{l^*}} s_{y_{l^*}, x_{k^*}^{l^*}}}_{\text{intended signal, } d} + \underbrace{\sqrt{\frac{p^{(b)}}{\mathcal{U}}} d_{y_{l^*}, x_{k^*}^{l^*}}^{-\frac{\beta}{2}} \boldsymbol{g}_{y_{l^*}, x_{k^*}^{l^*}} \sum_{k=1, k \ne k^*}^{\mathcal{U}} \boldsymbol{v}_{y_{l^*}, x_k^{l^*}} s_{y_{l^*}, x_k^{l^*}}}_{\text{multi-user interference, } dd} \\ & + \underbrace{\sqrt{\frac{p^{(b)}}{\mathcal{U}}} \sum_{y_l \in \Phi^{(b)} \setminus \{y_{l^*}\}} d_{y_l, x_{k^*}^{l^*}}^{-\frac{\beta}{2}} \boldsymbol{g}_{y_l, x_{k^*}^{l^*}} \boldsymbol{V}_{y_l} \boldsymbol{s}_{y_l}}_{\text{inter-cell interference, } d \to d} + \underbrace{\sum_{x_k^l \in \tilde{\Phi}^{(u)} \setminus \{x_{k^*}^{l^*}\}} \sqrt{p_{x_k^l}^{(u)}} d_{x_k^l, x_{k^*}^{l^*}}^{-\frac{\beta}{2}} h_{x_k^l, x_{k^*}^{l^*}} s_{x_k^l}}_{\text{cross-mode interference, } u \to d} \\ & + \underbrace{\sqrt{p_{x_{k^*}^{l^*}}^{(u)}} h_{x_{k^*}^{l^*}, x_{k^*}^{l^*}} s_{x_{k^*}^{l^*}}}_{\text{self-interference, } si \to d} + \underbrace{\eta_{x_{k^*}^{l^*}}}_{\text{noise}} \end{aligned} \tag{3}$$

where $p^{(b)}$ is the BS total transmit power, $\tilde{\Phi}^{(u)}$ ($\subset \Phi^{(u)}$) is the set of scheduled UEs locations, $p_{x_k^l}^{(u)}$ is the l-th BS k-th scheduled UE transmit power for sending $s_{x_k^l}$, and $\eta_{x_{k^*}^{l^*}}$ is the complex additive white Gaussian noise (AWGN) at UE k^* with mean zero and variance σ_d^2, respectively.

Next, let $\boldsymbol{H}_{y_l} = [\boldsymbol{h}_{x_k^l, y_l}]_{1 \le k \le \mathcal{U}} \in \mathcal{C}^{N_r \times \mathcal{U}}$ represent the compound UL channel matrix at the l-BS from its $\mathcal{U}$ scheduled UEs. The linear receiver filter at the l-th BS is denoted using $\boldsymbol{W}_{y_l} = [\boldsymbol{w}_{x_k^l, y_l}^T]_{1 \le k \le \mathcal{U}}^T \in \mathcal{C}^{\mathcal{U} \times N_r}$. The corresponding post-processing UL signal can be written as

$$\begin{aligned} y_u = & \underbrace{\sqrt{p_{x_{k^*}^{l^*}}^{(u)}} d_{x_{k^*}^{l^*}, y_{l^*}}^{-\frac{\beta}{2}} \boldsymbol{w}_{x_{k^*}^{l^*}, y_{l^*}}^T \boldsymbol{h}_{x_{k^*}^{l^*}, y_{l^*}} s_{x_{k^*}^{l^*}}}_{\text{intended signal, } u} + \underbrace{\sum_{k=1, k \ne k^*}^{\mathcal{U}} \sqrt{p_{x_k^{l^*}}^{(u)}} d_{x_k^{l^*}, y_{l^*}}^{-\frac{\beta}{2}} \boldsymbol{w}_{x_{k^*}^{l^*}, y_{l^*}}^T \boldsymbol{h}_{x_k^{l^*}, y_{l^*}} s_{x_k^{l^*}}}_{\text{multi-user interference, } uu} \\ & + \underbrace{\sum_{x_k^l \in \tilde{\Phi}^{(u)} \setminus \{\forall x_k^{l^*}\}} \sqrt{p_{x_k^l}^{(u)}} d_{x_k^l, y_{l^*}}^{-\frac{\beta}{2}} \boldsymbol{w}_{x_{k^*}^{l^*}, y_{l^*}}^T \boldsymbol{h}_{x_k^l, y_{l^*}} s_{x_k^l}}_{\text{inter-cell interference, } u \to u} + \underbrace{\sqrt{\frac{p^{(b)}}{\mathcal{U}}} \sum_{y_l \in \Phi^{(b)} \setminus \{y_{l^*}\}} d_{y_l, y_{l^*}}^{-\frac{\beta}{2}} \boldsymbol{w}_{x_{k^*}^{l^*}, y_{l^*}}^T \boldsymbol{G}_{y_l, y_{l^*}} \boldsymbol{V}_{y_l} \boldsymbol{s}_{y_l}}_{\text{cross-mode interference, } d \to u} \\ & + \underbrace{\sqrt{\frac{p^{(b)}}{\mathcal{U}}} \boldsymbol{w}_{x_{k^*}^{l^*}, y_{l^*}}^T \boldsymbol{G}_{y_{l^*}, y_{l^*}} \boldsymbol{V}_{y_{l^*}} \boldsymbol{s}_{y_{l^*}}}_{\text{self-interference, } si \to u} + \underbrace{\boldsymbol{w}_{x_{k^*}^{l^*}, y_{l^*}}^T \boldsymbol{\eta}_{y_{l^*}}}_{\text{noise}} \end{aligned} \tag{4}$$

where $\boldsymbol{\eta}_{y_{l^*}} \in \mathcal{C}^{N_r \times 1}$ is the AWGN vector with mean zero and covariance matrix $\sigma_u^2 \mathbf{I}_{N_r}$.

It is improtant to note that the set of scheduled UEs is *strictly not* an indpendent process due to the spatial dependencies arising from (i) the cellular association strategy, and (ii) the constraint of each BS serving multiple UEs per resource block [30], [31]. For the sake of mathematical tractability, in the same spirit as in [32], we invoke the following assumption.

Assumption 1. *The set of scheduled UEs $\tilde{\Phi}^{(u)}$, conditioned on the spatial constraints imposed by the cellular association strategy and the number of UEs being served by each BS per resource block, is modeled as an independent stationary PPP with density $\lambda^{(u)}$.*

The multi-user interference can be supressed using ZF under perfect CSI. However, SI can severely limit performance particularly in the UL. In the DL, we adopt a linear ZF-SIN precoder where the transmit antenna array ($N_t \geq N_r + \mathcal{U}$) is utilized to jointly suppress multi-user interference and SI at the receiving antennas. This is achieved at BS l by setting the columns of $\boldsymbol{V}_{y_l}$ equal to the normalized columns of $\hat{\boldsymbol{G}}^{+}_{y_l} = \hat{\boldsymbol{G}}^{\dagger}_{y_l}(\hat{\boldsymbol{G}}_{y_l}\hat{\boldsymbol{G}}^{\dagger}_{y_l})^{-1} = [\hat{\boldsymbol{g}}_{y_l,x^l_k}]_{1\leq k\leq \mathcal{U}} \in \mathcal{C}^{N_t\times\mathcal{U}}$ where $\hat{\boldsymbol{G}}_{y_l} = \boldsymbol{G}_{y_l}(\mathbf{I}_{N_t} - \boldsymbol{G}^{\dagger}_{y_l,y_l}(\boldsymbol{G}_{y_l,y_l}\boldsymbol{G}^{\dagger}_{y_l,y_l})^{-1}\boldsymbol{G}_{y_l,y_l})$. Note the proposed alignment-based precoder differs from the extended ZF scheme in [21] where 'all-zero' streams are sent for suppressing SI. In the UL, a linear ZF decoder, eliminating multi-user interference, is employed with the normalized rows of $\boldsymbol{H}^{+}_{y_l} = (\boldsymbol{H}^{\dagger}_{y_l}\boldsymbol{H}_{y_l})^{-1}\boldsymbol{H}^{\dagger}_{y_l} = [\hat{\boldsymbol{h}}^{T}_{x^l_k,y_l}]^{T}_{1\leq k\leq\mathcal{U}} \in \mathcal{C}^{\mathcal{U}\times N_r}$ set as the row vectors of $\boldsymbol{W}_{y_l}$, at the BS l.

The received signal-to-interference-plus-noise ratio (SINR) in the DL is given by

$$\gamma_d = \frac{\mathcal{X}_d}{\mathcal{I}_{d\to d} + \mathcal{I}_{u\to d} + \mathcal{I}_{si\to d} + \sigma_d^2} \tag{5}$$

where $\mathcal{X}_d = \frac{p^{(b)}}{\mathcal{U}} d^{-\beta}_{y_{l^*},x^{l^*}_{k^*}} G_{y_{l^*},x^{l^*}_{k^*}}$, $\mathcal{I}_{d\to d} = \frac{p^{(b)}}{\mathcal{U}} \sum_{y_l\in\Phi^{(b)}\setminus\{y_{l^*}\}} d^{-\beta}_{y_l,x^{l^*}_{k^*}} G_{y_l,x^{l^*}_{k^*}}$, $\mathcal{I}_{u\to d} = \sum_{x^l_k\in\tilde{\Phi}^{(u)}\setminus\{x^{l^*}_{k^*}\}} p^{(u)}_{x^l_k} d^{-\beta}_{x^l_k,x^{l^*}_{k^*}} H_{x^l_k,x^{l^*}_{k^*}}$, $\mathcal{I}_{si\to d} = p^{(u)}_{x^{l^*}_{k^*}} H_{x^{l^*}_{k^*},x^{l^*}_{k^*}}$, $G_{y_{l^*},x^{l^*}_{k^*}} \triangleq |\boldsymbol{g}_{y_{l^*},x^{l^*}_{k^*}}\boldsymbol{v}_{y_{l^*},x^{l^*}_{k^*}}|^2$, $G_{y_l,x^{l^*}_{k^*}} \triangleq \|\boldsymbol{g}_{y_l,x^{l^*}_{k^*}}\boldsymbol{V}_{y_l}\|^2$, $H_{x^l_k,x^{l^*}_{k^*}} \triangleq |h_{x^l_k,x^{l^*}_{k^*}}|^2$, and $H_{x^{l^*}_{k^*},x^{l^*}_{k^*}} \triangleq |h_{x^{l^*}_{k^*},x^{l^*}_{k^*}}|^2$. The ZF-SIN vector $\boldsymbol{v}_{y_{l^*},x^{l^*}_{k^*}} = \hat{\boldsymbol{g}}_{y_{l^*},x^{l^*}_{k^*}}/\|\hat{\boldsymbol{g}}_{y_{l^*},x^{l^*}_{k^*}}\|$ is selected in the direction of the projection of $\boldsymbol{g}_{y_{l^*},x^{l^*}_{k^*}}$ on $\text{Null}([\boldsymbol{g}_{y_{l^*},x^{l^*}_{k}}]_{1\leq k\leq\mathcal{U},k\neq k^*}, \boldsymbol{G}_{y_{l^*},y_{l^*}})$. The nullspace spanned by the multi-user interference and SI is $D_d \triangleq N_t - N_r - \mathcal{U} + 1$ dimensional. For tractability's sake, we assume the outer-cell precoding matrices have independent column vectors, thus $G_{y_l,x^{l^*}_{k^*}} \approx \sum_{k=1}^{\mathcal{U}} |\boldsymbol{g}_{y_l,x^{l^*}_{k^*}}\boldsymbol{v}_{y_l,x^l_k}|^2$ [32], [33]. The channel power gain from each interfering BS in the DL is hence interpreted as the aggregation of multiple separate beams from the projection of the cross-link channel vector $\boldsymbol{g}_{y_l,x^{l^*}_{k^*}}$ onto the one-dimensional precoding vectors $\boldsymbol{v}_{y_l,x^l_k}$, $1\leq k\leq\mathcal{U}$. The scheduled UEs, on the other hand, transmit using single-antennas (in all directions).

Assumption 2. *Considering isotropic Rayleigh fading and perfect CSI, the channel power gains at the reference UE x_{k^*}, from the intended BS y_{l^*}, interfering BS y_l, and scheduled UE x^l_k, are respectively $G_{y_{l^*},x^{l^*}_{k^*}} \sim$ Gamma$(D_d,1)$, $G_{y_l,x^{l^*}_{k^*}} \approx$ Gamma$(\mathcal{U},1)$, and $H_{x^l_k,x^{l^*}_{k^*}} \sim$ Gamma$(1,1)$.*

The Rayleigh fading model is applicable to cases without line-of-sight (LOS), e.g., under rich multipath and afar transceiver distance. In FD, where the nodes transmit and receive antennas are in the vicinity of each other, the SI cannot generally be characterized by the Rayleigh distribution. The Rician fading model which takes into account the different LOS and scattered paths can hence be invoked to capture performance under generalized SI cancellation capability [8].

Assumption 3. *The SI channel $h_{x^{l^*}_{k^*},x^{l^*}_{k^*}}$ envelope follows a Rician distribution with Rician factor $K = \frac{\mu^2}{2\upsilon^2}$ (dominant over scattered paths ratio) and fading attenuation $\Omega = \mu^2 + 2\upsilon^2$ (variance). The SI channel power gain is a non-central Chi-squared random variable where*

$$\mathcal{P}_{H_{(.)}}(h) = \frac{1+K}{\Omega}\exp\left(-\left(K + \frac{(1+K)h}{\Omega}\right)\right) I_0\left(2\sqrt{\frac{K(1+K)h}{\Omega}}\right) {}_0\tilde{F}_1\left(;1;\left(\frac{K(1+K)h}{\Omega}\right)\right) \tag{6}$$

and

$$\mathcal{M}_{H_{(.)}}(z) = \frac{1+K}{1+K+z\Omega}\exp\left(-\frac{zK\Omega}{1+K+z\Omega}\right). \tag{7}$$

Next, we express the received SINR from the reference UE at its serving BS as

$$\gamma_u = \frac{\mathcal{X}_u}{\mathcal{I}_{u\to u} + \mathcal{I}_{d\to u} + \sigma_u^2} \tag{8}$$

where we have $\mathcal{X}_u = p^{(u)}_{x^{l^*}_{k^*}} d^{-\beta}_{x^{l^*}_{k^*},y_{l^*}} H_{x^{l^*}_{k^*},y_{l^*}}$, $\mathcal{I}_{u\to u} = \sum_{x^l_k\in\tilde{\Phi}^{(u)}\setminus\{\forall x^{l^*}_k\}} p^{(u)}_{x^l_k} d^{-\beta}_{x^l_k,y_{l^*}} H_{x^l_k,y_{l^*}}$, $\mathcal{I}_{d\to u} = \frac{p^{(b)}}{\mathcal{U}} \sum_{y_l\in\Phi^{(b)}\setminus\{y_{l^*}\}} d^{-\beta}_{y_l,y_{l^*}} G_{y_l,y_{l^*}}$, $H_{x^{l^*}_{k^*},y_{l^*}} \triangleq |\boldsymbol{w}^T_{x^{l^*}_{k^*},y_{l^*}}\boldsymbol{h}_{x^{l^*}_{k^*},y_{l^*}}|^2$, $H_{x^l_k,y_{l^*}} \triangleq |\boldsymbol{w}^T_{x^{l^*}_{k^*},y_{l^*}}\boldsymbol{h}_{x^l_k,y_{l^*}}|^2$, and $G_{y_l,y_{l^*}} \triangleq \|\boldsymbol{w}^T_{x^{l^*}_{k^*},y_{l^*}}\boldsymbol{G}_{y_l,y_{l^*}}\boldsymbol{V}_{y_l}\|^2$. Note $\|\hat{\boldsymbol{h}}^T_{x^{l^*}_{k^*},y_{l^*}}\|^{-2} = \{(\boldsymbol{H}^{\dagger}_{y_{l^*}}\boldsymbol{H}_{y_{l^*}})^{-1}\}_{k^*,k^*} \sim \text{Erlang}(D_u,1)$ where $D_u \triangleq N_r - \mathcal{U} + 1$. In turn, $\boldsymbol{W}_{y_{l^*}}$ is selected independently from $\boldsymbol{h}_{x^l_k,y_{l^*}}$ and $\boldsymbol{G}_{y_l,y_{l^*}}$. By recalling the assumption that $\boldsymbol{V}_{y_l}$ has independent column vectors, $G_{y_l,y_{l^*}} \approx \sum_{k=1}^{\mathcal{U}} |\boldsymbol{w}^T_{x^{l^*}_{k^*},y_{l^*}}\boldsymbol{G}_{y_l,y_{l^*}}\boldsymbol{v}_{y_l,k}|^2$.

Assumption 4. *Considering isotropic Rayleigh channels and perfect CSI, the channel power gains for the reference UE x_{k^*}, interfering scheduled UE x^l_k, and interfering BS y_l are respectively modeled using $H_{x^{l^*}_{k^*},y_{l^*}} \sim$ Gamma$(D_u,1)$, $H_{x^l_k,y_{l^*}} \sim$ Gamma$(1,1)$, and $G_{y_l,y_{l^*}} \approx$ Gamma$(\mathcal{U},1)$.*

IV. Self-Interference-Aware Power Control

Power control has been pivotal in the proliferation of cellular networks. A particular focus is on the UL due to the UEs' limited number of antennas and power budget, and the more complex nature of the interference versus the DL. In long-term-evolution (LTE)-Advanced, UL fractional power control is defined to tackle the path-loss effect [34]. Recently, interference-aware fractional power control has been proposed to ensure that the power adjustment intended for path-loss compensation does not cause undesired interference to neighboring nodes [35]. Intuitively, power control has perhaps an even more essential role to play in FD cellular setups. This topic remains largely unexplored.

In this work, we propose an LTE-Advanced compliant SIA fractional power control mechanism where the UEs adjust their transmit power based on the distance-dependent path-loss, SI, and maximum available transmit power. The motivation behind this is in line with the argument that the UEs with limited number of antennas rely on digital/analog domain interference cancellation strategies, and hence may experience severe SI affecting the DL operation. Here, specifically, an arbitrary scheduled UE k transmits to its serving BS (say l) using

$$p_{x_k^l}^{(u)} = \min\left(p_0 d_{x_k^l, y_l}^{\psi\beta}, I_{\text{SI}} H_{x_k^l, x_k^l}^{-1}, p^{(u)}\right) \tag{9}$$

where p_0, ψ ($\in (0,1]$), I_{SI}, and $p^{(u)}$ are respectively the normalized power density, compensation factor, tolerable SI level, and maximum transmit power at the UE [32]. The value of I_{SI} can be set as the difference in the noise floor power from the gain of the UE SI cancellation capability. Note that the above is a generalization of the existing approaches for UL power control including total (without I_{SI}) and truncated (without I_{SI} and $p^{(u)}$) fractional power control schemes.

Lemma 1. *The c.d.f. and p.d.f. expressions for the transmit power of a typical UE under the SIA fractional power control mechanism are respectively*

$$\mathcal{F}_{p_{x_k^l}^{(u)}}(p) = \left(1 - \exp\left(-\Xi_{\text{I}}(p)\right)\left(1 - Q_1\left(\sqrt{2K}, \sqrt{2(1+K)\Xi_{\text{II}}(p)}\right)\right)\right)\left(1 - \mathcal{H}\left(p - p^{(u)}\right)\right) + \mathcal{H}\left(p - p^{(u)}\right) \tag{10}$$

and

$$\mathcal{P}_{p_{x_k^l}^{(u)}}(p) = \begin{cases} \exp\left(-\Xi_{\text{I}}\left(p^{(u)}\right)\right)\left(1 - Q_1\left(\sqrt{2K}, \sqrt{2(1+K)\Xi_{\text{II}}\left(p^{(u)}\right)}\right)\right)\delta\left(p - p^{(u)}\right) & p \geq p^{(u)} \\ \dfrac{\exp\left(-\Xi_{\text{I}}(p)\right)}{p}\left[\dfrac{2\Xi_{\text{I}}(p)}{\psi\beta}\left(1 - Q_1\left(\sqrt{2K}, \sqrt{2(1+K)\Xi_{\text{II}}(p)}\right)\right) + (1+K)\Xi_{\text{II}}(p)\right. & \\ \left.\times \exp\left(-\left(K + (1+K)\Xi_{\text{II}}(p)\right)\right) {}_0\tilde{F}_1\left(;1;K(1+K)\Xi_{\text{II}}(p)\right)\right] & p < p^{(u)} \end{cases} \tag{11}$$

where $\Xi_{\text{I}}(p) = \pi\lambda^{(b)}\left(\frac{p}{p_0}\right)^{\frac{2}{\psi\beta}}$ *and* $\Xi_{\text{II}}(p) = \frac{I_{SI}}{p\Omega}$.
Proof: See Appendix A.

The computation of the functions of SINR, such as SE, can be greatly simplified with a non-direct approach using only the moments of the random variables involved [36]. On the other hand, the p.d.f. expression in (11), is a highly non-linear piecewise function. Hence, the exact higher-order statistics of the proposed SIA fractional power control mechanism required for the calculation of SE cannot be derived in closed-form. In what follows, however, we develop results for the positive moments of the UEs transmit power in certain special cases where the corresponding p.d.f. has a more tractable form.

Corollary 1. *For the special case of no LOS path SI channel ($K \to 0$)*

$$\mathcal{P}^{(K\to 0)}_{p_{x_k^l}^{(u)}}(p) = \begin{cases} \exp\left(-\Xi_{\text{I}}\left(p^{(u)}\right)\right)\left(1 - \exp\left(-\Xi_{\text{II}}\left(p^{(u)}\right)\right)\right)\delta\left(p - p^{(u)}\right) & p \geq p^{(u)} \\ \dfrac{\exp\left(-\Xi_{\text{I}}(p)\right)}{p}\left(\dfrac{2\Xi_{\text{I}}(p)}{\psi\beta}\left(1 - \exp\left(-\Xi_{\text{II}}(p)\right)\right) + \Xi_{\text{II}}(p)\exp\left(-\Xi_{\text{II}}(p)\right)\right) & p < p^{(u)}. \end{cases} \tag{12}$$

In the special case of no distance-dependent path-loss compensation ($p_0 \to +\infty$)

$$\mathcal{P}^{(p_0\to+\infty)}_{p_{x_k^l}^{(u)}}(p) = \begin{cases} \left(1 - Q_1\left(\sqrt{2K}, \sqrt{2(1+K)\Xi_{\text{II}}\left(p^{(u)}\right)}\right)\right)\delta\left(p - p^{(u)}\right) & p \geq p^{(u)} \\ (1+K)\Xi_{\text{II}}\left(p^2\right)\exp\left(-\left(K + (1+K)\Xi_{\text{II}}(p)\right)\right) {}_0\tilde{F}_1\left(;1;K(1+K)\Xi_{\text{II}}(p)\right) & p < p^{(u)}. \end{cases} \tag{13}$$

In the special case without a constraint on the SI ($I_{SI} \to +\infty$)

$$\mathcal{P}^{(I_{SI}\to+\infty)}_{p_{x_k^l}^{(u)}}(p) = \begin{cases} \left(1 - \exp\left(-\Xi_{\text{I}}\left(p^{(u)}\right)\right)\right)\delta\left(p - p^{(u)}\right) & p \geq p^{(u)} \\ \dfrac{2\Xi_{\text{I}}(p)}{\psi\beta p}\exp\left(-\Xi_{\text{I}}(p)\right) & p < p^{(u)}. \end{cases} \tag{14}$$

Lemma 2. *The $\flat$-th positive moment of the SIA transmit power admits a closed-form expression without a constraint on the transmit power ($p^{(u)} \to +\infty$), no LOS path SI channel, full-compensation ($\psi \to 1$), and path-loss exponent of four ($\beta \to 4$)*

$$\mathbb{E}^{(P^{(u)}\to+\infty,K\to 0,\psi\to 1,\beta\to 4)}\left\{{p_{x_k^l}^{(u)}}^{\flat}\right\} = \frac{\hat{\Xi}_{\mathrm{II}}^{\flat}}{\sqrt{\pi}}\left(\mathcal{G}_{0,3}^{3,0}\left(\left.{}_{-\flat+1,0,\frac{1}{2}}\right|\frac{\hat{\Xi}_{\mathrm{I}}^2\hat{\Xi}_{\mathrm{II}}}{4}\right)\right. \\ \left. - \frac{\hat{\Xi}_{\mathrm{I}}\sqrt{\hat{\Xi}_{\mathrm{II}}}}{2}\mathcal{G}_{0,3}^{3,0}\left(\left.{}_{-\flat-\frac{1}{2},0,\frac{1}{2}}\right|\frac{\hat{\Xi}_{\mathrm{I}}^2\hat{\Xi}_{\mathrm{II}}}{4}\right)\right) + \frac{(2\flat)!}{\hat{\Xi}_{\mathrm{I}}^{2\flat}} \quad (15)$$

where $\hat{\Xi}_{\mathrm{I}} = \frac{\pi\lambda^{(b)}}{p_0^{\frac{2}{\beta\psi}}}$ (here $= \frac{\pi\lambda^{(b)}}{\sqrt{p_0}}$) and $\hat{\Xi}_{\mathrm{II}} = \frac{I_{SI}}{\Omega}$. The corresponding average transmit power is

$$\mathbb{E}^{(-''-)}\left\{p_{x_k^l}^{(u)}\right\} = \frac{\hat{\Xi}_{\mathrm{II}}}{\sqrt{\pi}}\left(\mathcal{G}_{0,3}^{3,0}\left(\left.{}_{0,0,\frac{1}{2}}\right|\frac{\hat{\Xi}_{\mathrm{I}}^2\hat{\Xi}_{\mathrm{II}}}{4}\right) - \frac{\hat{\Xi}_{\mathrm{I}}\sqrt{\hat{\Xi}_{\mathrm{II}}}}{2}\mathcal{G}_{0,3}^{3,0}\left(\left.{}_{-\frac{3}{2},0,\frac{1}{2}}\right|\frac{\hat{\Xi}_{\mathrm{I}}^2\hat{\Xi}_{\mathrm{II}}}{4}\right)\right) + \frac{2}{\hat{\Xi}_{\mathrm{I}}^2}. \quad (16)$$

With no distance-dependent path-loss compensation and limit on the transmit power

$$\mathbb{E}^{(p_0\to+\infty,P^{(u)}\to+\infty)}\left\{{p_{x_k^l}^{(u)}}^{\flat}\right\} = (1+K)^{\flat}\hat{\Xi}_{\mathrm{II}}^{\flat}\Gamma(1-\flat)\,{}_1F_1(\flat;1;-K). \quad (17)$$

For no LOS path SI channel under this setup, we have

$$\mathbb{E}^{(-''-,K\to 0)}\left\{{p_{x_k^l}^{(u)}}^{\flat}\right\} = \hat{\Xi}_{\mathrm{II}}^{\flat}\Gamma(1-\flat). \quad (18)$$

Under the special case without limits on the transmit power and SI, we have

$$\mathbb{E}^{(I_{SI}\to+\infty,P^{(u)}\to+\infty)}\left\{{p_{x_k^l}^{(u)}}^{\flat}\right\} = \frac{\Gamma\left(\frac{\psi\beta\flat}{2}+1\right)}{\hat{\Xi}_{\mathrm{I}}^{\frac{\psi\beta\flat}{2}}}. \quad (19)$$

With path-loss exponent of four and compensation factor of one

$$\mathbb{E}^{(-''-,K\to 0)}\left\{{p_{x_k^l}^{(u)}}^{\flat}\right\} = \frac{2}{\hat{\Xi}_{\mathrm{I}}^2}. \quad (20)$$

Proof: See Appendix B.

V. Spectral Efficiency Analysis

The notion of doubling the SE by going from HD to FD has been a key driving force behind the surge of interest in this topic. This is however only a theoretical upper-bound concerning point-to-point nodes with perfect SI cancellation capability. In the context of multi-cell environments, many factors come into play, such as increased interference complexity and intensity, which requires rigorous investigation prior to branding large-scale FD as a solution for 5G and beyond.

In order to facilitate performance analysis and optimization, we provide a framework for the computation of the DL and UL SEs in the FD massive MIMO cellular network. We utilize a m.g.f.-based methodology, which avoids the need for the direct computation of the SINR p.d.f. and only requires the m.g.f.s of the different signals involved [37], [38].

Lemma 3. *The DL and UL SEs in the FD massive MIMO cellular network are respectively*

$$\mathcal{S}_{d,f} = \mathbb{E}\left\{\log_2\left(1+\gamma_d\right)\right\} = \log_2(e)\int_0^{+\infty}\int_0^{+\infty}\mathcal{M}_{\mathcal{I}_{si\to d}|p}(z)\mathcal{M}_{\mathcal{I}_{u\to d}|p}(z)\int_0^{+\infty}\left(1-\mathcal{M}_{\mathcal{X}_{d}|r}(z)\right) \\ \times\,\mathcal{M}_{\mathcal{I}_{d\to d}|r}(z)\frac{\exp\left(-z\sigma_d^2\right)}{z}\mathcal{P}_{p_{x_k^l}^{(u)}}(p)\,\mathcal{P}_{d_{x_{k^*}^{l^*},y_{l^*}}}(r)\,\mathrm{d}z\,\mathrm{d}r\,\mathrm{d}p \quad (21)$$

and

$$\mathcal{S}_{u,f} = \mathbb{E}\left\{\log_2\left(1+\gamma_u\right)\right\} = \log_2(e)\int_0^{+\infty}\mathcal{M}_{\mathcal{I}_{d\to u}}(z)\int_0^{+\infty}\int_0^{+\infty}\left(1-\mathcal{M}_{\mathcal{X}_u|p,r}(z)\right)\mathcal{M}_{\mathcal{I}_{u\to u}|p,r}(z) \\ \times\,\frac{\exp\left(-z\sigma_u^2\right)}{z}\mathcal{P}_{p_{x_k^l}^{(u)}}(p)\,\mathcal{P}_{d_{y_{l^*},x_{k^*}^{l^*}}}(r)\,\mathrm{d}z\,\mathrm{d}r\,\mathrm{d}p. \quad (22)$$

Proof: The proof follows directly from [37, Lemma 1] and is omitted due to space limitations.

Next, we provide explicit expressions for the conditional m.g.f.s of all signals involved.

Lemma 4. *The conditional m.g.f.s of the different signals required for the calculation of the FD massive MIMO cellular network DL and UL SEs are given by*

$$\mathcal{M}_{\mathcal{X}_d|r}(z) = \left(1 + z\frac{p^{(b)}}{\mathcal{U}} r^{-\beta}\right)^{-D_d}, \tag{23}$$

$$\mathcal{M}_{\mathcal{X}_u|p,r}(z) = \left(1 + zpr^{-\beta}\right)^{-D_u}, \tag{24}$$

$$\mathcal{M}_{\mathcal{I}_{d\to d}|r}(z) = \exp\Bigg(- \pi\lambda^{(b)} \Bigg[r^2 \left(\left(z\frac{p^{(b)}}{\mathcal{U}} r^{-\beta} + 1 \right)^{-\mathcal{U}} - 1 \right) + \Gamma\left(\mathcal{U} + \frac{2}{\beta}\right) \left(z\frac{p^{(b)}}{\mathcal{U}} \right)^{-\mathcal{U}} \times \left(\left(z\frac{p^{(b)}}{\mathcal{U}} \right)^{\mathcal{U}+\frac{2}{\beta}} \frac{\Gamma\left(1 - \frac{2}{\beta}\right)}{\Gamma(\mathcal{U})} - \mathcal{U} r^{\mathcal{U}\beta+2} \, {}_2\tilde{F}_1 \left(\mathcal{U}+1, \mathcal{U}+\frac{2}{\beta}; \mathcal{U}+\frac{2}{\beta}+1; -\frac{r^\beta}{z\frac{p^{(b)}}{\mathcal{U}}} \right) \right) \Bigg] \Bigg), \tag{25}$$

$$\mathcal{M}_{\mathcal{I}_{u\to u}|p,r} = \exp\Bigg(- \pi\mathcal{U}\lambda^{(b)} \Bigg[(zp)^{\frac{2}{\beta}} \Gamma\left(1 - \frac{2}{\beta}\right) \Gamma\left(1 + \frac{2}{\beta}\right) - r^2 \left(1 - \frac{2r^\beta}{zp(\beta+2)} \, {}_2F_1 \left(1, 1 + \frac{2}{\beta}; 2 + \frac{2}{\beta}; -\frac{r^\beta}{zp} \right) \right) \Bigg] \Bigg), \tag{26}$$

$$\mathcal{M}_{\mathcal{I}_{u\to d}|p}(z) = \exp\left(-\pi\mathcal{U}\lambda^{(b)} (zp)^{\frac{2}{\beta}} \Gamma\left(1 - \frac{2}{\beta}\right) \Gamma\left(1 + \frac{2}{\beta}\right) \right), \tag{27}$$

$$\mathcal{M}_{\mathcal{I}_{d\to u}}(z) = \exp\left(-\pi\lambda^{(b)} \left(z\frac{p^{(b)}}{\mathcal{U}} \right)^{\frac{2}{\beta}} \frac{\Gamma\left(1 - \frac{2}{\beta}\right) \Gamma\left(\mathcal{U} + \frac{2}{\beta}\right)}{\mathcal{U}^{\frac{2}{\beta}} \Gamma(\mathcal{U})} \right), \tag{28}$$

and

$$\mathcal{M}_{\mathcal{I}_{si\to d}|p}(z) = \frac{1+K}{1+K+zp\Omega} \exp\left(-\frac{zpK\Omega}{1+K+zp\Omega} \right). \tag{29}$$

Proof: See Appendix C.

It is very important to highlight that the outer-cell UL interference in (26) is derived by taking into account the spatial constraints from *Assumption 1* using a spatially-thinned PPP [32], [39]. The cross-mode interference at the reference UE in (27), on the other hand, is from all other scheduled UEs, and is hence approximated using a PPP based on *Assumption 1*.

In certain special cases, the signals m.g.f.s can be simplified further as in the following result.

Corollary 2. *For the special UL case with path-loss exponent being equal to four*

$$\mathcal{M}^{(\beta\to4)}_{\mathcal{I}_{u\to u}|p,r} = \exp\left(-\pi\mathcal{U}\lambda^{(b)} \sqrt{zp} \arctan\left(\frac{\sqrt{zp}}{r^2} \right) \right) \tag{30}$$

and

$$\mathcal{M}^{(\beta\to4)}_{\mathcal{I}_{u\to d}|p}(z) = \exp\left(-\frac{\pi^2}{2}\mathcal{U}\lambda^{(b)} \sqrt{zp} \right). \tag{31}$$

For the special DL case with single-user SISO and path-loss exponent being equal to four

$$\mathcal{M}^{(\mathcal{U}\to1,\beta\to4)}_{\mathcal{I}_{d\to d}|r} = \exp\left(-\pi\lambda^{(b)} \sqrt{zp^{(b)}} \arctan\left(\frac{\sqrt{zp^{(b)}}}{r^2} \right) \right) \tag{32}$$

and

$$\mathcal{M}^{(\mathcal{U}\to1,\beta\to4)}_{\mathcal{I}_{d\to u}}(z) = \exp\left(-\frac{\pi^2}{2}\lambda^{(b)} \sqrt{zp^{(b)}} \right). \tag{33}$$

The cross-mode interference can be further simplified under special power control cases

$$\mathcal{M}^{(p^{(u)}\to+\infty,K\to0,\beta\to4,\psi\to1)}_{\mathcal{I}_{u\to d}}(z) = \frac{1}{1 + \frac{\pi}{2}\sqrt{zp_0}} + \frac{1}{\sqrt{\pi}} \mathcal{G}^{3,0}_{0,3}\left({}_{0,\frac{1}{2},1} \middle| \hat{\Xi}_{\mathrm{II}} \left(\frac{\mathcal{U}\hat{\Xi}_{\mathrm{I}}}{2} \left(1 + \frac{\pi}{2}\sqrt{zp_0} \right) \right)^2 \right)$$

$$- \frac{\mathcal{U}\tilde{\Xi}_{\mathrm{I}}\sqrt{\tilde{\Xi}_{\mathrm{II}}}}{2\sqrt{\pi}}\mathcal{G}_{0,3}^{3,0}\left({}_{-\frac{1}{2},0,\frac{1}{2}} \middle| \hat{\Xi}_{\mathrm{II}}\left(\frac{\mathcal{U}\hat{\Xi}_{\mathrm{I}}}{2}\left(1+\frac{\pi}{2}\sqrt{zp_0}\right)\right)^2\right), \quad (34)$$

$$\mathcal{M}_{\mathcal{I}_{u\to d}}^{(p^{(u)}\to+\infty,K\to 0,\beta\to 4,\psi\to 1)}(z) = \frac{1}{\sqrt{\pi}}\mathcal{G}_{0,3}^{3,0}\left({}_{0,\frac{1}{2},1} \middle| z\hat{\Xi}_{\mathrm{II}}\left(\frac{\pi^2\mathcal{U}\lambda^{(b)}}{4}\right)^2\right), \quad (35)$$

and

$$\mathcal{M}_{\mathcal{I}_{u\to d}}^{(p^{(u)}\to+\infty,K\to 0,\beta\to 4,\psi\to 1)}(z) = \frac{1}{1+\frac{\pi}{2}\sqrt{zp_0}}. \quad (36)$$

Proof: See Appendix C.

The SE expressions in (21) and (22) require three-fold integral computations - as opposed to the manifold integrals involved in the direct p.d.f.-based approach. Next, we show that it is possible to further reduce the computational complexity in certain special cases.

Corollary 3. *For the special case with single-antenna, single-user, no LOS path SI channel, interference-limited DL/UL region ($\sigma_d^2\to 0,\sigma_u^2\to 0$), and path-loss exponent being equal to four, the above can be be reduced to double-integrals expressions ($\omega=\frac{p^{(b)}}{p}$ for DL and $\omega=\frac{p}{p^{(b)}}$ for UL, respectively)*

$$\mathcal{S}_{\{.\},f}^{(N^t=1,N^r=1,\mathcal{U}=1,K\to 0,\sigma_d^2\to 0,\sigma_u^2\to 0,\beta\to 4)} = \log_2(e)\int_0^{+\infty}\int_0^{+\infty}\frac{2\pi\lambda^{(b)}}{\sqrt{\Omega}\left(1+s^2\right)}\sqrt{\omega}$$
$$\times\Bigg[\sin\left(\frac{\pi\lambda^{(b)}}{\sqrt{\Omega}}\left(\frac{\pi}{2}+\sqrt{\omega}\left(s+\operatorname{arccot}(s)\right)\right)\right)\mathscr{C}\left(\frac{\pi\lambda^{(b)}}{\sqrt{\Omega}}\left(\frac{\pi}{2}+\sqrt{\omega}\left(s+\operatorname{arccot}(s)\right)\right)\right)$$
$$+\cos\left(\frac{\pi\lambda^{(b)}}{\sqrt{\Omega}}\left(\frac{\pi}{2}+\sqrt{\omega}\left(s+\operatorname{arccot}(s)\right)\right)\right)\left(\frac{\pi}{2}-\mathscr{S}\left(\frac{\pi\lambda^{(b)}}{\sqrt{\Omega}}\left(\frac{\pi}{2}+\sqrt{\omega}\left(s+\operatorname{arccot}(s)\right)\right)\right)\right)\Bigg]\mathcal{P}_{p_{x_k^l}^{(u)}}(p)\,\mathrm{d}s\,\mathrm{d}p. \quad (37)$$

Further considering the special case where the receivers can remove SI entirely (SI $\to 0$), we can develop ($\omega=\frac{p^{(b)}}{p}$ for DL and $\omega=\frac{p}{p^{(b)}}$ for UL, respectively)

$$\mathcal{S}^{(-''-,SI\to 0)} = \log_2(e)\int_0^{+\infty}\int_0^{+\infty}\frac{2}{\left(1+s^2\right)\left(\frac{\pi}{2\sqrt{\omega}}+s+\operatorname{arccot}(s)\right)}\mathcal{P}_{p_{x_k^l}^{(u)}}(p)\,\mathrm{d}s\,\mathrm{d}p. \quad (38)$$

For the special case without path-loss compensation and limit on the transmit power, the SE expressions in (38) can be reduced to single-fold integrals

$$\mathcal{S}_{d,f}^{(-''-,p_0\to+\infty,p^{(u)}\to+\infty)} = \log_2(e)\int_0^{+\infty}\frac{2}{\left(1+s^2\right)\left(s+\operatorname{arccot}(s)\right)}\Bigg[1-\frac{\pi\sqrt{\pi}}{2\left(s+\operatorname{arccot}(s)\right)}\sqrt{\frac{I_{SI}}{p^{(b)}\Omega}}$$
$$-\left(\frac{\pi}{2\left(s+\operatorname{arccot}(s)\right)}\right)^2\frac{I_{SI}}{p^{(b)}\Omega}\exp\left(-\left(\frac{\pi}{2\left(s+\operatorname{arccot}(s)\right)}\right)^2\frac{I_{SI}}{p^{(b)}\Omega}\right)$$
$$\left(Ei\left(\left(\frac{\pi}{2\left(s+\operatorname{arccot}(s)\right)}\right)^2\frac{I_{SI}}{p^{(b)}\Omega}\right)-\pi erfi\left(\frac{\pi}{2\left(s+\operatorname{arccot}(s)\right)}\sqrt{\frac{I_{SI}}{p^{(b)}\Omega}}\right)\right)\Bigg]\,\mathrm{d}s \quad (39)$$

and

$$\mathcal{S}_{u,f}^{(-''-)} = \log_2(e)\int_0^{+\infty}\frac{4}{\pi\left(1+s^2\right)}\sqrt{\frac{I_{SI}}{p^{(b)}\Omega}}\Bigg[\sqrt{\pi}+\frac{2\left(s+\operatorname{arccot}(s)\right)}{\pi}\sqrt{\frac{I_{SI}}{p^{(b)}\Omega}}\exp\Bigg(-\left(\frac{2\left(s+\operatorname{arccot}(s)\right)}{\pi}\right)^2$$
$$\times\frac{I_{SI}}{p^{(b)}\Omega}\Bigg)\left(Ei\left(\left(\frac{2\left(s+\operatorname{arccot}(s)\right)}{\pi}\right)^2\frac{I_{SI}}{p^{(b)}\Omega}\right)-\pi erfi\left(\frac{2\left(s+\operatorname{arccot}(s)\right)}{\pi}\sqrt{\frac{I_{SI}}{p^{(b)}\Omega}}\right)\right)\Bigg]\,\mathrm{d}s. \quad (40)$$

On the other hand, considering no constraints on the SI and the transmit power, the SE expressions in (38) can be reduced to single-fold integrals

$$\mathcal{S}_{d,f}^{(-''-,I_{SI}\to+\infty,p^{(u)}\to+\infty)} = \log_2(e)\int_0^{+\infty} -\frac{4\lambda^{(b)}}{1+s^2}\sqrt{\frac{p^{(b)}}{p_0}}\exp\left(2\lambda^{(b)}\left(s+\operatorname{arccot}(s)\right)\sqrt{\frac{p^{(b)}}{p_0}}\right) Ei\left(-2\lambda^{(b)}\left(s+\operatorname{arccot}(s)\right)\sqrt{\frac{p^{(b)}}{p_0}}\right)\mathrm{d}s \quad (41)$$

and

$$\mathcal{S}_{u,f}^{(-''-)} = \log_2(e)\int_0^{+\infty}\frac{2}{(1+s^2)\left(s+\operatorname{arccot}(s)\right)}\left[1+\frac{\pi^2\lambda^{(b)}}{2\left(s+\operatorname{arccot}(s)\right)}\sqrt{\frac{p^{(b)}}{p_0}} \times\exp\left(\frac{\pi^2\lambda^{(b)}}{2\left(s+\operatorname{arccot}(s)\right)}\sqrt{\frac{p^{(b)}}{p_0}}\right) Ei\left(-\frac{\pi^2\lambda^{(b)}}{2\left(s+\operatorname{arccot}(s)\right)}\sqrt{\frac{p^{(b)}}{p_0}}\right)\right]\mathrm{d}s. \quad (42)$$

Proof: See Appendix D.

VI. Full-Duplex versus Half-Duplex

It should be noted that the SE expressions provided greatly facilitate performance analysis and optimization for generalized FD cellular deployments. At the same time, the framework can serve as a benchmark tool for comparing the performance of FD over HD. Although an explicit expression for the corresponding gain cannot be obtained due to the highly complex SE expressions involving multiple improper integrals, we do provide results in certain special cases. In what follows, $\mathcal{S}_{d,h}$ and $\mathcal{S}_{u,h}$ are respectively used to denote the SEs of a typical UE in the DL and the UL of a HD cellular system. For comparison of FD and HD modes, we consider the SE over two time slots, i.e., $\mathbb{S}_f = 2(\mathcal{S}_{d,f}+\mathcal{S}_{u,f})$ for FD, and $\mathbb{S}_h = \mathcal{S}_{d,h}+\mathcal{S}_{u,h}$ for HD, respectively.

Lemma 5. *For the special case with single-antenna, single-user, fixed UL transmit power $p^{(u)}$, and complete SI removal, the following joint DL/UL SE expressions over two time slots can be respectively derived for the FD and HD cases*

$$\mathbb{S}_f^{(N^t\to1,N^r\to1,\mathcal{U}\to1,SI\to0,K\to0,\beta\to4)} = \log_2(e)\int_0^{+\infty}\frac{\frac{2\pi}{1+s^2}\left(\sqrt{\frac{p^{(u)}}{p^{(b)}}}+\sqrt{\frac{p^{(b)}}{p^{(u)}}}\right)+8(s+\operatorname{arccot}(s))}{\left(\frac{\pi}{2}\sqrt{\frac{p^{(u)}}{p^{(b)}}}+s+\operatorname{arccot}(s)\right)\left(\frac{\pi}{2}\sqrt{\frac{p^{(b)}}{p^{(u)}}}+s+\operatorname{arccot}(s)\right)}\,\mathrm{d}s \quad (43)$$

and

$$\mathbb{S}_h^{(N^t\to1,N^r\to1,\mathcal{U}\to1,\beta\to4)} = \log_2(e)\int_0^{+\infty}\frac{4}{(1+s^2)\left(s+\operatorname{arccot}(s)\right)}\,\mathrm{d}s. \quad (44)$$

We develop bounded solutions respectively for the above (with real domain $\left(\frac{\pi}{8-\pi}\right)^2 < \frac{p^{(b)}}{p^{(u)}} < \left(\frac{8-\pi}{\pi}\right)^2$ or $\left(\frac{\pi}{8-\pi}\right)^2 < \frac{p^{(u)}}{p^{(b)}} < \left(\frac{8-\pi}{\pi}\right)^2$, otherwise the real-part of (45) holds the solution)

$$\tilde{\mathbb{S}}_f^{(-''-)} \le 2\log_2(e)\left(\Psi\left(\frac{8}{\pi\left(1+\sqrt{\frac{p^{(u)}}{p^{(b)}}}\right)}-1\right)+\Psi\left(\frac{8}{\pi\left(1+\sqrt{\frac{p^{(b)}}{p^{(u)}}}\right)}-1\right)\right) \quad (45)$$

and

$$\tilde{\mathbb{S}}_h^{(-''-)} \le 2\log_2(e)\Psi\left(\frac{8}{\pi}-1\right) \quad (46)$$

where

$$\Psi(\alpha) = \frac{(1+\alpha)\left((5-\alpha)\operatorname{arccot}\left(\sqrt{\alpha}\right)+\sqrt{\alpha}\log\left(\frac{1}{4}(1+\alpha)\right)\right)-\frac{\pi}{2}(5-4\sqrt{\alpha}+\alpha)(1-2\sqrt{\alpha}-\alpha)}{\frac{\sqrt{\alpha}}{1+\alpha}(25-6\alpha+\alpha^2)}. \quad (47)$$

Proof: See Appendix E.

Note the HD SE in Lemma 5 is independent of the system parameters. The exact and bounded SEs over two time slots (in nat/s/Hz) are approximately 3 and 2.72, from (44) and (45), respectively. On the other hand, the FD SE in (43) is a function of the DL/UL transmit powers only. Hence, consider the problem of finding the optimal fixed transmit power values which results in the highest FD over HD SE gain

$$\underset{p^{(b)},p^{(u)}}{\text{maximize}} \quad \frac{\mathbb{S}_f}{\mathbb{S}_h} \qquad \text{subject to:} \quad p^{(b)}>0 \text{ and } p^{(u)}>0. \quad (48)$$

The rate in the HD case, $\mathbb{S}_h$, is concave in $p^{(b)} > 0$ and $p^{(u)} > 0$. On the other hand, it can be shown that $\mathbb{S}_f$ is strictly quasi-convex in $p^{(b)} > 0$ and $p^{(u)} > 0$, i.e., the achievable rate in the FD case strictly increases, or first decreases and then strictly increases in $p^{(b)}$ and $p^{(u)}$. The objective function in (48) is in turn strictly quasi-convex in the set $p^{(b)} > 0$ and $p^{(u)} > 0$. This guarantees the existence of a unique maximum solution under a positive transmit power region. $\mathbb{S}_h$ and $\mathbb{S}_f$, however, are highly non-linear functions involving multiple improper integrals. Thus, an exact closed-form solution cannot be obtained. Further, the functions derivatives are unavailable analytically, and their accurate computation, e.g., using finite-differences, is difficult. Heuristic-based methods, such as downhill simplex [40] with penalty function, can therefore be applied to solve the problem. We do however provide a tight bounded solution in the following special case.

Lemma 6. *Consider the lower-bound SEs in Lemma 5. The multi-variable optimization problem for the FD over HD SE gain in (48) is equivalent to the following with the ratio of the fixed transmit powers being the single optimization variable*

$$\underset{x=\frac{p^{(b)}}{p^{(u)}}}{\textit{maximize}} \quad \frac{\mathbb{S}_f}{\mathbb{S}_h} = \frac{\Psi\left(\frac{8}{\pi\left(1+\sqrt{x}\right)}-1\right)+\Psi\left(\frac{8}{\pi\left(1+\frac{1}{\sqrt{x}}\right)}-1\right)}{\Psi\left(\frac{8}{\pi}-1\right)} \quad \textit{subject to:} \quad \left(\frac{\pi}{\pi-8}\right)^2 < x < \left(\frac{\pi-8}{\pi}\right)^2. \tag{49}$$

The solution to the above problem is given by

$$x^* = 1, \quad \left(\frac{\mathbb{S}_f}{\mathbb{S}_h}\right)^* = \frac{2\Psi\left(\frac{4}{\pi}-1\right)}{\Psi\left(\frac{8}{\pi}-1\right)} = 1 + 13\left(\frac{1}{10^2}\right) + \frac{1}{2}\left(\frac{1}{10^4}\right). \tag{50}$$

Proof: See Appendix F.

For the special SISO case described in Lemma (5), the highest exact and bounded SE percentage gains from the FD over the HD are respectively $\sim$9% and $\sim$13% (same values also hold for individual gains in the DL and the UL). It can therefore be inferred that without advanced techniques for tackling the inter-cell interference, even under perfect SI cancellation capability, the FD operation with SISO achieves only minor improvements in terms of SE over HD.

VII. Numerical Results

In this section, we provide several numerical examples in order to assess the performance of the FD massive MIMO cellular network under different system settings. MC simulations are accordingly provided for the purpose of examining the validity of the proposed analytical framework. The BS deployment density is considered to be $\lambda^{(b)} = \frac{4}{\pi}$ per unit area (km$\times$km). The total system bandwidth is taken to be $B = 20$ MHz. The noise power is calculated using $\sigma^2 = -170 + 10\log_{10}(B) + N_f$ (dBm), where N_f is the noise figure. The maximum available transmit powers at the BSs and UEs are set to 43 dBm and 23 dBm, respectively. Note that the results from the MC simulations are obtained from 10^4 trials in a circular region of radius 10^2 km, considering (i) PPP under spatial constraints for the scheduled UEs (*Assumption 1*), (ii) non-central Chi-squared distribution for the SI channel power gain (*Assumption 3*), and (iii) Gamma distribution for the other channels power gains (*Assumptions 2 and 4*).

1) Different FD Cellular Setups: We compare the DL and UL performance of several different FD cellular networks, namely, LSAS (Massive MIMO), MIMO, and SISO, in Fig. 1. The results confirm prior findings that the UL rate is the main performance bottleneck in FD cellular systems with baseline single-antenna transmission. Furthermore, it can be observed that significant performance gains can be achieved by exploiting the large scale antenna array with linear ZF-SIN precoding and linear ZF receive combining. For example, with $\beta = 4$, the UL SE in the proposed massive MIMO cellular setup is more than 96 times greater than that in the SISO case. By increasing the antenna array size, further improvements can be realized from (i) the added DoF, and (ii) the potential to linearly reduce the transmit powers of the BSs and UEs without degrading the received signal-to-noise ratio (SNR). These aspects are studied further in this section. Note that the MC results confirm the validity of the proposed analytical framework.

2) FD versus HD Massive MIMO: Next, we investigate the performance of the FD massive MIMO cellular network with respect to its HD counterpart over a wide range of UE SI channel attenuations in Fig. 2. It can be seen that any potential improvements from the FD operation occurs for SI channel attenuation well below -80 dB. This trend indicates that without advanced SI mitigation solutions being available at the terminals, the conventional HD cellular LSAS is arguably the more sensible deployment choice. With nearly perfect SI cancellation at the reference UE, on the other hand, the maximum system SE gain in the FD massive MIMO cellular network over its analogous HD variant here is 47% with $\mathcal{U} = 1$ (resulting from 73% and 1% increase in the DL and UL SEs, respectively).

3) Transmit/Receive Antenna Array Size: The impact of different number of transmit and receive antennas on the SE gain of the massive MIMO-enabled FD system over its HD counterpart is depicted in Fig. 3. It can be observed that the corresponding performance gain increases by adding more transmit antennas due to the less significant loss of diversity from utilizing the ZF-SIN precoding scheme. For smaller transmit antenna arrays, however, increasing the number of receive antennas may degrade the relative improvement from the FD operation over HD mode. It is also important to note that the relative FD over

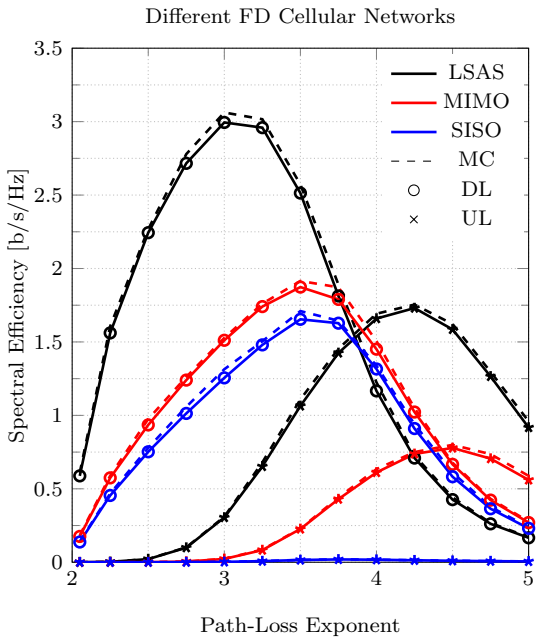

Fig. 1. System parameters are: $\lambda^{(b)} = \frac{4}{\pi}$ BSs/km^2, LSAS ($N_t = 80$, $N_r = 20$, $\mathcal{U} = 8$, $p^{(b)} = 30$ dBm), MIMO ($N_t = 16$, $N_r = 8$, $\mathcal{U} = 4$, $p^{(b)} = 43$ dBm), SISO ($N_t = 1$, $N_r = 1$, $\mathcal{U} = 1$, $p^{(b)} = 43$ dBm), $p^{(u)} = 23$ dBm, $p_0 = -80$ dBm, $B = 20$ MHz, $N_f = 10$ dB, $\psi = 1$, $\Omega = -80$ dB, $K = 1$.

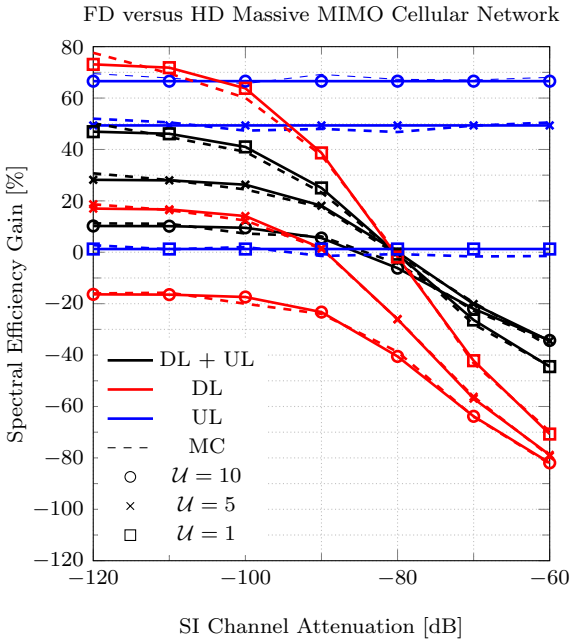

Fig. 2. System parameters are: $\lambda^{(b)} = \frac{4}{\pi}$ BSs/km^2, $N_t = 350$, $N_r = 50$, $p^{(b)} = 30$ dBm, $p^{(u)} = 23$ dBm, $p_0 = -80$ dBm, $B = 20$ MHz, $N_f = 10$ dB, $\beta = 4$, $\psi = 1$, $K = 1$.

HD massive MIMO gain improves in the path-loss severity. The optimal ratio of transmit over receive antennas, on the other hand, depends on the particular system settings. A rigorous study of this aspect is postponed to future work.

4) Transmit Power Budget: It has been shown in [2] that under perfect CSI, the transmit energy can be linearly conserved in the number of antennas. This is a contributing factor in tackling the UL rate bottleneck, as was demonstrated in Fig. 2. We depict the impact of different BS transmit power and UE maximum transmit power in Fig. 4. Intuitively, increasing $P^{(b)}$, or $P^{(u)}$, respectively improves the corresponding SE in the DL, or the UL; the relative gain however decreases for larger power budgets. Further, the DL and UL SEs are conflicting functions in the BS/UE transit powers. In general, we observe that a large difference in the DL/UL power levels is deteriorating to the overall performance in FD mode. Due to the large disparity in the DL/UE SEs, however, the direct optimization of the FD sum-rate places the focus on the DL, see Fig. 4. It can therefore

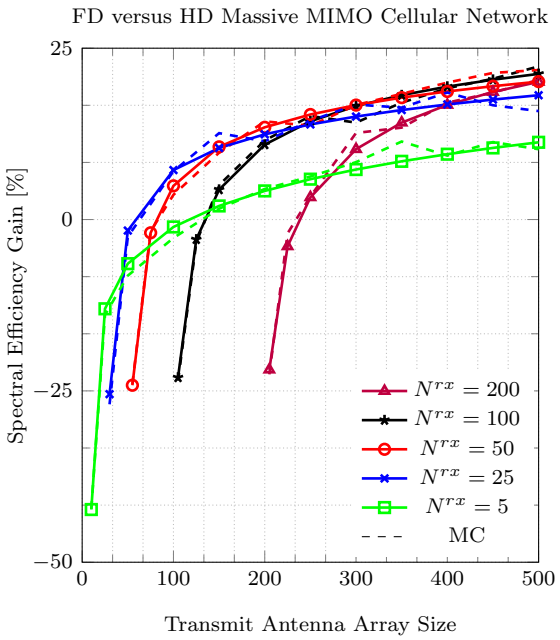

Fig. 3. System parameters are: $\lambda^{(b)} = \frac{4}{\pi}$ BSs/km^2, $\mathcal{U} = 5$, $p^{(b)} = 30$ dBm, $p^{(u)} = 23$ dBm, $p_0 = -80$ dBm, $B = 20$ MHz, $N_f = 10$ dB, $\beta = 4$, $\psi = 1$, $\Omega = -90$ dB, $K = 2$.

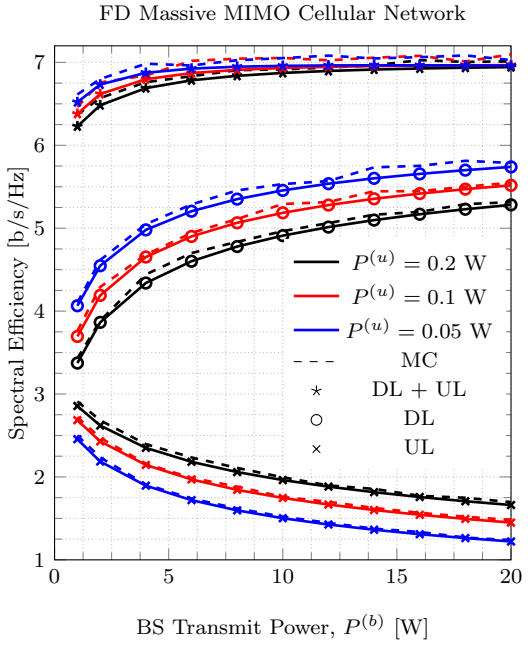

Fig. 4. System parameters are: $\lambda^{(b)} = \frac{4}{\pi}$ BSs/km^2, $N_t = 250$, $N_r = 50$, $\mathcal{U} = 6$, $p_0 = -80$ dBm, $B = 20$ MHz, $N_f = 10$ dB, $\beta = 4$, $\psi = 1$, $\Omega = -100$ dB, $K = 1$.

be inferred that the optimization problem should be tackled by applying a weight to the UL SE. This is however beyond the scope of this work.

5) Uplink Power Control: The results presented so far were based on the conventional UL fractional power control mechanism defined in the existing LTE standards for HD cases. Next, we study the performance of the massive MIMO-enabled FD cellular network with different fixed (at maximum power), conventional, and proposed SIA fractional power control protocols under different SI channel attenuations in Fig. 5. It can be observed that the lack of self-interference-awareness in the case of fixed as well as fractional power allocation strategies means that the DL performance significantly suffers in the case of large SI channel attenuations. The proposed scheme can therefore serve as an important safe-guard mechanism for ensuring that a certain maximum SI level is not exceeded.

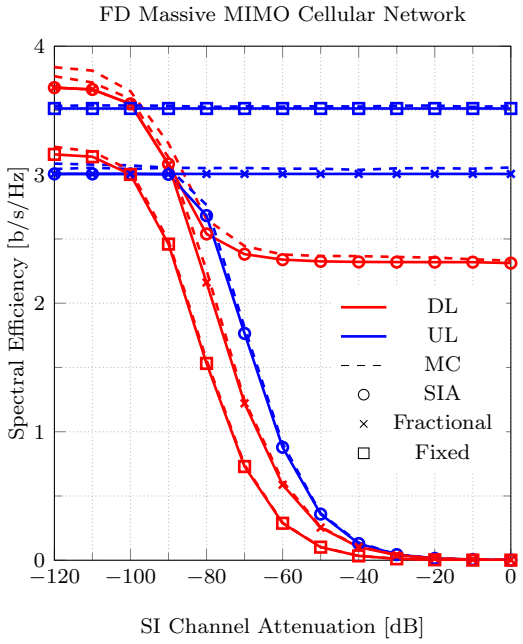

Fig. 5. System parameters are: $\lambda^{(b)} = \frac{4}{\pi}$ BSs/km^2, $N_t = 150$, $N_r = 50$, $\mathcal{U} = 4$, $p^{(b)} = 30$ dBm, $p^{(u)} = 23$ dBm, $p_0 = -80$ dBm, $\frac{I_{\text{SI}}}{\sigma^2} = 25$ dB, $p_f^{(u)} = 23$ dBm, $B = 20$ MHz, $N_f = 10$ dB, $\beta = 4$, $\psi = 1$, $K = 0$.

VIII. Summary

We provided a theoretical framework using tools from stochastic geometry and point processes for the study of massive MIMO-enabled FD multi-cell multi-user cellular networks. The DL and UL SEs with linear ZF-SIN precoding, SIA fractional power control, and linear ZF receiver were characterized over Rician SI and Rayleigh intended and other-interference fading channels. The results highlighted the promising potential of massive MIMO towards unlocking the UL rate bottleneck in FD communication systems. The SE gain of the FD massive MIMO cellular network over its HD counterpart was on the other hand shown to be largely dependent on the SI cancellation capability of the UEs.

References

[1] F. Boccardi, R. W. Heath, A. Lozano, T. L. Marzetta, and P. Popovski, "Five disruptive technology directions for 5G," *IEEE Commun. Mag.*, vol. 52, no. 2, pp. 74–80, Feb. 2014.

[2] H. Q. Ngo, E. G. Larsson, and T. L. Marzetta, "Energy and spectral efficiency of very large multiuser MIMO systems," *IEEE Trans. Commun.*, vol. 61, no. 4, pp. 1436–1449, Apr. 2013.

[3] P. Patcharamaneepakorn, S. Wu, C. X. Wang, H. Aggoune, M. Alwakeel, X. Ge, and M. Di Renzo, "Spectral, energy and economic efficiency of 5G multi-cell massive MIMO systems with generalized spatial modulation," *IEEE Trans. Veh. Technol.*, accepted 2016.

[4] S. Goyal, C. Galiotto, N. Marchetti, and S. Panwar, "Throughput and coverage for a mixed full and half duplex small cell network," *arXiv:1602.09115*, 2016.

[5] M. Duarte, C. Dick, and A. Sabharwal, "Experiment-driven characterization of full-duplex wireless systems," *IEEE Trans. Wireless Commun.*, vol. 11, no. 12, pp. 4296–4307, Dec. 2012.

[6] E. Everett, A. Sahai, and A. Sabharwal, "Passive self-interference suppression for full-duplex infrastructure nodes," *IEEE Trans. Wireless Commun.*, vol. 13, no. 2, pp. 680–694, Feb. 2014.

[7] M. Chung, M. S. Sim, J. Kim, D. K. Kim, and C. B. Chae, "Prototyping real-time full duplex radios," *IEEE Commun. Mag.*, vol. 53, no. 9, pp. 56–63, Sept. 2015.

[8] D. Kim, H. Lee, and D. Hong, "A survey of in-band full-duplex transmission: From the perspective of PHY and MAC layers," *IEEE Commun. Surveys Tuts.*, vol. 17, no. 4, pp. 2017–2046, Fourth Quart. 2015.

[9] D. Nguyen, L. N. Tran, P. Pirinen, and M. Latva-aho, "On the spectral efficiency of full-duplex small cell wireless systems," *IEEE Trans. Wireless Commun.*, vol. 13, no. 9, pp. 4896–4910, Sept. 2014.

[10] I. Atzeni and M. Kountouris, "Full-duplex MIMO small-cell networks: Performance analysis," *arXiv:1504.04167*, 2015.

[11] G. Zhang, K. Yang, P. Liu, and J. Wei, "Power allocation for full-duplex relaying-based D2D communication underlaying cellular networks," *IEEE Trans. Veh. Technol.*, vol. 64, no. 10, pp. 4911–4916, Oct. 2015.

[12] N. Pappas, M. Kountouris, A. Ephremides, and A. Traganitis, "Relay-assisted multiple access with full-duplex multi-packet reception," *IEEE Trans. Wireless Commun.*, vol. 14, no. 7, pp. 3544–3558, July 2015.

[13] M. Mohammadi, B. K. Chalise, H. A. Suraweera, C. Zhong, G. Zheng, and I. Krikidis, "Throughput analysis and optimization of wireless-powered multiple antenna full-duplex relay systems," *IEEE Trans. Commun.*, vol. 64, no. 4, pp. 1769–1785, Apr. 2016.

[14] M. Mohammadi, H. A. Suraweera, and C. Tellambura, "Full-duplex cloud-RAN with uplink/downlink remote radio head association," *arXiv:1602.08836*, 2016.

[15] A. AlAmmouri, H. ElSawy, O. Amin, and M. Alouini, "In-band full-duplex communications for cellular networks with partial uplink/downlink overlap," *arXiv:1508.02909*, 2015.

[16] A. Sadeghi, M. Luvisotto, F. Lahouti, S. Vitturi, and M. Zorzi, "Statistical QoS analysis of full duplex and half duplex heterogeneous cellular networks," *arXiv:1604.00588*, 2016.

[17] L. Wang, F. Tian, T. Svensson, D. Feng, M. Song, and S. Li, "Exploiting full duplex for device-to-device communications in heterogeneous networks," *IEEE Commun. Mag.*, vol. 53, no. 5, pp. 146–152, May 2015.
[18] A. AlAmmouri, H. ElSawy, and M. S. Alouini, "Flexible design for α-duplex communications in multi-tier cellular networks," *IEEE Trans. Commun.*, vol. 64, no. 8, pp. 3548–3562, Aug. 2016.
[19] A. Sabharwal, P. Schniter, D. Guo, D. W. Bliss, S. Rangarajan, and R. Wichman, "In-band full-duplex wireless: Challenges and opportunities," *IEEE J. Sel. Areas Commun.*, vol. 32, no. 9, pp. 1637–1652, Sept. 2014.
[20] G. Y. Li, M. Bennis, and G. Yu, "Full duplex communications [guest editorial]," *IEEE Commun. Mag.*, vol. 53, no. 5, p. 90, May 2015.
[21] B. Yin, M. Wu, C. Studer, J. R. Cavallaro, and J. Lilleberg, "Full-duplex in large-scale wireless systems," in *Proc. Asilomar Conf. Signals, Syst. and Comput. (ASILOMAR)*, Nov. 2013, pp. 1623–1627.
[22] K. Min, S. Park, Y. Jang, T. Kim, and S. Choi, "Antenna ratio for sum-rate maximization in full-duplex large-array base station with half-duplex multi-antenna users," *IEEE Trans. Veh. Technol.*, accepted 2016.
[23] Y.-G. Lim, D. Hong, and C.-B. Chae, "Performance analysis of self-interference cancellation methods in full-duplex large-scale MIMO systems," *arXiv:1508.02166*, 2015.
[24] S. Huberman and T. Le-Ngoc, "Full-duplex MIMO precoding for sum-rate maximization with sequential convex programming," *IEEE Trans. Veh. Technol.*, vol. 64, no. 11, pp. 5103–5112, Nov. 2015.
[25] J. Kim, W. Choi, and H. Park, "Beamforming for full-duplex multiuser MIMO systems," *IEEE Trans. Veh. Technol.*, accepted 2016.
[26] L. Wang, K. K. Wong, M. Elkashlan, A. Nallanathan, and S. Lambotharan, "Secrecy and energy efficiency in massive MIMO aided heterogeneous C-RAN: A new look at interference," *IEEE J. Sel. Topics Signal Process.*, accepted, 2016.
[27] G. Caire, N. Jindal, M. Kobayashi, and N. Ravindran, "Multiuser MIMO achievable rates with downlink training and channel state feedback," *IEEE Trans. Inf. Theory*, vol. 56, no. 6, pp. 2845–2866, June 2010.
[28] A. Shojaeifard, K. A. Hamdi, E. Alsusa, D. K. C. So, and J. Tang, "A unified model for the design and analysis of spatially-correlated load-aware HetNets," *IEEE Trans. Commun.*, vol. 62, no. 11, pp. 1–16, Nov. 2014.
[29] F. Boccardi, J. Andrews, H. Elshaer, M. Dohler, S. Parkvall, P. Popovski, and S. Singh, "Why to decouple the uplink and downlink in cellular networks and how to do it," *IEEE Commun. Mag.*, vol. 54, no. 3, pp. 110–117, Mar. 2016.
[30] T. D. Novlan, H. S. Dhillon, and J. G. Andrews, "Analytical modeling of uplink cellular networks," *IEEE Trans. Wireless Commun.*, vol. 12, no. 6, pp. 2669–2679, June 2013.
[31] H. Y. Lee, Y. J. Sang, and K. S. Kim, "On the uplink SIR distributions in heterogeneous cellular networks," *IEEE Commun. Lett.*, vol. 18, no. 12, pp. 2145–2148, Dec. 2014.
[32] M. D. Renzo and P. Guan, "Stochastic geometry modeling and system-level analysis of uplink heterogeneous cellular networks with multi-antenna base stations," *IEEE Trans. Commun.*, vol. 64, no. 6, pp. 2453–2476, June 2016.
[33] A. Shojaeifard, K. A. Hamdi, E. Alsusa, D. K. C. So, J. Tang, and K. K. Wong, "Design, modeling, and performance analysis of multi-antenna heterogeneous cellular networks," *IEEE Trans. Commun.*, vol. 64, no. 7, pp. 3104–3118, July 2016.
[34] S. Parkvall, A. Furuskar, and E. Dahlman, "Evolution of LTE toward IMT-advanced," *IEEE Commun. Mag.*, vol. 49, no. 2, pp. 84–91, Feb. 2011.
[35] F. J. Martin-Vega, G. Gomez, M. C. Aguayo-Torres, and M. Di Renzo, "Analytical modeling of interference aware power control for the uplink of heterogeneous cellular networks," *arXiv:1601.03164*, 2016.
[36] A. Shojaeifard, K. A. Hamdi, E. Alsusa, D. K. C. So, and J. Tang, "Exact SINR statistics in the presence of heterogeneous interferers," *IEEE Trans. Inform. Theory*, vol. 61, no. 12, pp. 6759–6773, Dec. 2015.
[37] K. Hamdi, "A useful lemma for capacity analysis of fading interference channels," *IEEE Trans. Commun.*, vol. 58, no. 2, pp. 411–416, Feb. 2010.
[38] M. Di Renzo, A. Guidotti, and G. Corazza, "Average rate of downlink heterogeneous cellular networks over generalized fading channels: A stochastic geometry approach," *IEEE Trans. Commun.*, vol. 61, no. 7, pp. 3050–3071, July 2013.
[39] T. Bai and R. W. Heath, "Analyzing uplink SINR and rate in massive MIMO systems using stochastic geometry," *IEEE Trans. Commun.*, accepted 2016.
[40] J. A. Nelder and R. Mead, "A simplex method for function minimization," *Comput. J.*, vol. 7, pp. 308–313, 1965.

APPENDIX A

The proposed SIA fractional power control mechanism c.d.f. can be expressed as

$$\mathcal{F}_{p^{(u)}_{x^l_k}}(p) = \left(1 - \mathcal{H}\left(p - p^{(u)}\right)\right) \mathscr{P}\left(\hat{p}^{(u)}_{x^l_k} \leq p\right) + \mathcal{H}\left(p - p^{(u)}\right) \tag{A.1}$$

where $\hat{p}^{(u)}_{x^l_k} = \min\left(p_0 d^{\psi\beta}_{x^l_k, y_l}, I_{\text{SI}} H^{-1}_{x^l_k, x^l_k}\right)$. Hence, we can write

$$\begin{aligned}\mathcal{F}_{\hat{p}^{(u)}_{x^l_k}}(p) &= \mathcal{F}_{p_0 d^{\psi\beta}_{x^l_k, y_l}}(p) + \mathcal{F}_{I_{\text{SI}} H^{-1}_{x^l_k, x^l_k}}(p) - \mathcal{F}_{p_0 d^{\psi\beta}_{x^l_k, y_l}}(p)\, \mathcal{F}_{I_{\text{SI}} H^{-1}_{x^l_k, x^l_k}}(p) \\ &= \mathscr{P}\left(d_{x^l_k, y_l} \leq \left(\frac{p}{p_0}\right)^{\frac{1}{\psi\beta}}\right) + \mathscr{P}\left(H_{x^l_k, x^l_k} \geq \frac{I_{\text{SI}}}{p}\right) - \mathscr{P}\left(d_{x^l_k, y_l} \leq \left(\frac{p}{p_0}\right)^{\frac{1}{\psi\beta}}\right) \mathscr{P}\left(H_{x^l_k, x^l_k} \geq \frac{I_{\text{SI}}}{p}\right). \end{aligned} \tag{A.2}$$

By considering the transmitter-receiver distance exponential distribution

$$\mathscr{P}\left(d_{x^l_k, y_l} \leq \left(\frac{p}{p_0}\right)^{\frac{1}{\psi\beta}}\right) = \int_0^{\left(\frac{p}{p_0}\right)^{\frac{1}{\psi\beta}}} 2\pi\lambda^{(b)} r \exp\left(-\pi\lambda^{(b)} r^2\right) \mathrm{d}r = 1 - \exp\left(-\pi\lambda^{(b)}\left(\frac{p}{p_0}\right)^{\frac{2}{\psi\beta}}\right), \tag{A.3}$$

and the SI channel power gain non-central Chi-squared distribution

$$\begin{aligned}\mathscr{P}\left(H_{x^l_k, x^l_k} \geq \frac{I_{\text{SI}}}{p}\right) &= \int_{\frac{I_{\text{SI}}}{p}}^{+\infty} \frac{1+K}{\Omega} \exp\left(-\left(K + \frac{(1+K)h}{\Omega}\right)\right) I_0\left(2\sqrt{\frac{K(1+K)h}{\Omega}}\right) \mathrm{d}h \\ &= Q_1\left(\sqrt{2K}, \sqrt{\frac{2(1+K)I_{\text{SI}}}{p\Omega}}\right), \end{aligned} \tag{A.4}$$

we can obtain

$$\mathcal{F}_{\hat{p}^{(u)}_{x^l_k}}(p) = 1 - \exp\left(-\pi\lambda^{(b)}\left(\frac{p}{p_0}\right)^{\frac{2}{\psi\beta}}\right)\left(1 - Q_1\left(\sqrt{2K}, \sqrt{\frac{2(1+K)I_{\text{SI}}}{p\Omega}}\right)\right). \tag{A.5}$$

We can write the following p.d.f. expression by differentiating the above

$$\mathcal{P}_{\hat{p}^{(u)}_{x^l_k}}(p) = \exp\left(-\pi\lambda^{(b)}\left(\frac{p}{p_0}\right)^{\frac{2}{\psi\beta}}\right)\left(\frac{2\pi\lambda^{(b)}}{\psi\beta p}\left(\frac{p}{p_0}\right)^{\frac{2}{\beta\psi}}\left(1 - Q_1\left(\sqrt{2K}, \sqrt{\frac{2(K+1)I_{\text{SI}}}{p\Omega}}\right)\right)\right.$$
$$\left. + \frac{(1+K)I_{\text{SI}}}{p^2\Omega}\exp\left(-\left(K + \frac{(1+K)I_{\text{SI}}}{p\Omega}\right)\right){}_0\tilde{F}_1\left(;1;\frac{K(1+K)I_{\text{SI}}}{p\Omega}\right)\right). \tag{A.6}$$

Hence, with some basic algebraic manipulations, we arrive at Lemma 1. ■

APPENDIX B

Consider the case where the p.d.f. of the transmit power is

$$\mathcal{P}^{(p^{(u)}\to+\infty, K\to 0, \beta\to 4, \psi\to 1)}_{p^{(u)}_{x^l_k}}(p) = \exp\left(-\pi\lambda^{(b)}\sqrt{\frac{p}{p_0}}\right)\left[\frac{2\pi\lambda^{(b)}}{4p}\sqrt{\frac{p}{p_0}}\left(1 - \exp\left(-\frac{I_{\text{SI}}}{p\Omega}\right)\right) + \frac{I_{\text{SI}}}{p^2\Omega}\exp\left(-\frac{I_{\text{SI}}}{p\Omega}\right)\right]. \tag{B.1}$$

By utilizing the integral identities (where $n > 0$ and $\flat > n$)

$$\int_0^{+\infty}\exp\left(-x^n\right)x^{\flat-n}\,\mathrm{d}x = \frac{\Gamma\left(\frac{1-n-\flat}{n}\right)}{n} \tag{B.2}$$

and

$$\int_0^{+\infty}\exp\left(-\sqrt{x} - \frac{1}{x}\right)x^{\flat-n}\,\mathrm{d}x = \frac{1}{\sqrt{\pi}}\mathcal{G}^{3,0}_{0,3}\left(\begin{matrix} \\ n-\flat-1, 0, \frac{1}{2}\end{matrix}\middle|\,\frac{1}{4}\right), \tag{B.3}$$

we can arrive at (15).

Next, consider the following transmit power p.d.f.

$$\mathcal{P}^{(p_0\to+\infty, p^{(u)}\to+\infty)}_{p^{(u)}_{x^l_k}}(p) = \frac{(1+K)I_{\text{SI}}}{p^2\Omega}\exp\left(-\left(K + \frac{(1+K)I_{\text{SI}}}{p\Omega}\right)\right){}_0\tilde{F}_1\left(;1;\frac{K(1+K)I_{\text{SI}}}{p\Omega}\right). \tag{B.4}$$

We derive the following integral identity (where $\flat < 1$ and $n > \flat$)

$$\int_0^{+\infty}\exp\left(\frac{1}{p}\right){}_0\tilde{F}_1\left(;1;\frac{1}{p}\right)p^{\flat-n}\;\mathrm{d}p = L_{\flat-n+1}(1)\Gamma(n-\flat-1). \tag{B.5}$$

Hence, by utilizing $\mathcal{L}_m(z) = {}_0\tilde{F}_1\left(-m;1;z\right)$, we can arrive at (17). It should be noted that with no path-loss compensation, the first and beyond positive moments ($\flat \geq 1$) of $p^{(u)}_{x^l_k}$ are infinite.

Finally, note the following unbounded transmit power p.d.f.

$$\mathcal{P}^{(p^{(u)}\to+\infty, I_{\text{SI}}\to 0)}_{p^{(u)}_{x^l_k}}(p) = \frac{2\pi\lambda^{(b)}}{\psi\beta p}\left(\frac{p}{p_0}\right)^{\frac{2}{\psi\beta}}\exp\left(-\pi\lambda^{(b)}\left(\frac{p}{p_0}\right)^{\frac{2}{\psi\beta}}\right). \tag{B.6}$$

By utilizing the integral identity (B.2), we can obtain (19). ■

APPENDIX C

Let Φ, λ, N, $\mathscr{E}$ denote the PPP, density, spatial DoF, and exclusion region radius, respectively. Hence, $\mathcal{I} = \sum_{x\in\Phi}P_xQ_x\|x\|^{-\beta}$ where x, P_x, Q_x are respectably the location, transmit power, and channel power gain of an arbitrary interferer with respect to a typical receiver assumed to be located at the origin. We proceed as follows

$$\mathcal{M}_{\mathcal{I}}(z) = \mathbb{E}\left\{\exp\left(-z\sum_{x\in\Phi}P_xQ_x\|x\|^{-\beta}\right)\right\} \overset{(i)}{=} \lim_{\mathscr{D}\to+\infty}\mathbb{E}_{\mathcal{N}}\left\{\left(\mathbb{E}_{P_x,Q_x,\|x\|}\left\{\exp\left(-zP_xQ_x\|x\|^{-\beta}\right)\right\}\right)^{\mathcal{N}}\right\}$$
$$\overset{(ii)}{=} \lim_{\mathscr{D}\to+\infty}\exp\left(\pi\lambda\left(\mathscr{D}^2 - \mathscr{E}^2\right)\left(\mathbb{E}_{P_x,Q_x,\|x\|}\left\{\exp\left(-zP_xQ_x\|x\|^{-\beta}\right)\right\} - 1\right)\right)$$

$$\overset{(iii)}{=} \lim_{\mathscr{D}\to+\infty} \exp\left(2\pi\lambda\mathbb{E}_{P_x,Q_x}\left(\int_{\mathscr{E}}^{\mathscr{D}} \mathcal{R}\left(\exp\left(-zP_xQ_x\|\mathcal{R}\|^{-\beta}-1\right)\right)\mathrm{d}\mathcal{R}\right)\right)$$
$$\overset{(iv)}{=} \exp\Bigg(-\pi\lambda\mathbb{E}_{P_x,Q_x}\left\{\left[\Gamma\left(1-\frac{2}{\beta}\right)-\Gamma\left(1-\frac{2}{\beta},zP_xQ_x\mathscr{E}^{-\beta}\right)\right](zP_xQ_x)^{\frac{2}{\beta}} + \mathscr{E}^2\left(\exp\left(-zP_xQ_x\mathscr{E}^{-\beta}\right)-1\right)\right\}\Bigg) \quad \text{(C.1)}$$

where (i) is written considering $\mathscr{N}$ conditional interferers are i.i.d. in a circular region of radius $\mathscr{D}$ ($>\mathscr{E}$) around the center with the limit as $\mathscr{D}\to+\infty$; (ii) is from characterizing $\mathscr{N}$ as a Poisson random variable with expected value $\pi\lambda\left(\mathscr{D}^2-\mathscr{E}^2\right)$ and hence utilizing the Poisson identity $\mathbb{E}\left\{\zeta^{\mathscr{N}}\right\}=\exp\left(\mathbb{E}\left\{\mathscr{N}\right\}(\zeta-1)\right)$; (iii) is written using the p.d.f. of the distance $\mathcal{R}$ (where $\mathscr{E}<\mathcal{R}<\mathscr{D}$)

$$\mathcal{P}_{\|x\|}(\mathcal{R})=\frac{2\mathcal{R}}{\mathscr{D}^2-\mathscr{E}^2}; \quad \text{(C.2)}$$

(iv) is obtained by invoking the integral identity (where $\alpha>0$ and $\beta>2$)

$$\mathbb{E}_{\|x\|}\left\{\exp\left(-\alpha\|x\|^{-\beta}\right)\right\}=\frac{2\alpha^{\frac{2}{\beta}}}{\beta\left(\mathscr{D}^2-\mathscr{E}^2\right)}\left[\Gamma\left(-\frac{2}{\beta},\frac{\alpha}{\mathscr{D}^\beta}\right)-\Gamma\left(-\frac{2}{\beta},\frac{\alpha}{\mathscr{E}^\beta}\right)\right], \quad \text{(C.3)}$$

and taking the limit as $\mathscr{D}\to+\infty$.

To proceed, the distribution of the channel power gain should be specified. Here, we consider the general case where $Q_x\sim\text{Gamma}(U,V)$, which can be used to capture a wide range of MIMO setups [38]. Hence, through utilizing the following integral identities (where $\alpha>0$ and $\beta>2$)

$$\mathbb{E}_{Q_x}\left\{Q_x^{\frac{2}{\beta}}\right\}=\frac{\Gamma\left(U+\frac{2}{\beta}\right)}{\Gamma(U)}V^{\frac{2}{\beta}}, \quad \text{(C.4)}$$

$$\mathbb{E}_{Q_x}\left\{\Gamma\left(1-\frac{2}{\beta},\alpha Q_x\right)\right\}=\frac{\Gamma\left(U-\frac{2}{\beta}+1\right)}{(\alpha V)^U\,\Gamma(U+1)}\,{}_2F_1\left(U,U-\frac{2}{\beta}+1;U+1;-\frac{1}{\alpha V}\right), \quad \text{(C.5)}$$

and

$$\mathbb{E}_{Q_x}\left\{\exp\left(-\alpha Q_x\right)\right\}=\frac{1}{(1+\alpha V)^U}, \quad \text{(C.6)}$$

we can arrive at

$$\mathcal{M}_{\mathcal{I}|P_x}(z)=\exp\Bigg(-\pi\lambda\Bigg[-\mathscr{E}^2+\frac{\mathscr{E}^2}{\left(zP_xV\mathscr{E}^{-\beta}+1\right)^U}+\frac{\Gamma\left(1-\frac{2}{\beta}\right)\Gamma\left(U+\frac{2}{\beta}\right)}{\Gamma\left(U\right)}\left(zP_xV\right)^{\frac{2}{\beta}} - \frac{U\beta}{U\beta+2}\frac{\mathscr{E}^{U\beta+2}}{\left(zP_xV\right)^U}\,{}_2F_1\left(U+1,U+\frac{2}{\beta};U+\frac{2}{\beta}+1;-\frac{\mathscr{E}^\beta}{zP_xV}\right)\Bigg]\Bigg). \quad \text{(C.7)}$$

Next, we require the distribution of the transmit power control mechanism under consideration. Here, we consider a SIA fractional power control mechanism $P_x=\min\left(p_0\mathcal{D}^{\psi\beta},I_{SI}Q_{x,x}^{-1},\mathscr{M}\right)$ where $\mathcal{D}$, $Q_{x,x}$, and $\mathscr{M}$ are respectively the normalized power density, transmitter-receiver distance, SI channel power gain, and maximum available transmit power. The corresponding pdf of P_x (derived in Lemma 1) is a highly non-linear piecewise function; as a result, an explicit expression for the average of (C.7) with respect to P_x cannot be derived.

For the special case where $\mathscr{E}\to0$, $K\to0$, $\beta\to4$, $\psi\to1$, and $\mathbb{M}\to+\infty$, we have the transmit power p.d.f. in (B.1) and the aggregate interference conditional m.g.f.

$$\mathcal{M}_{\mathcal{I}|P_x}^{(\mathscr{E}\to0,\beta\to4)}(z)=\exp\left(-\pi^{\frac{3}{2}}\lambda\frac{\Gamma\left(U+\frac{1}{2}\right)}{\Gamma(U)}\sqrt{zP_xV}\right). \quad \text{(C.8)}$$

Hence, by utilizing the integral identities developed in (B.2) and (B.3)

$$\mathcal{M}_{\mathcal{I}}^{(\mathscr{E}\to0,\mathscr{M}\to+\infty,K\to0,\beta\to4,\psi\to1)}(z)=\frac{1}{1+\frac{\Gamma\left(U+\frac{1}{2}\right)}{\Gamma(U)}\sqrt{\pi zp_0V}} + \frac{1}{\sqrt{\pi}}\mathcal{G}_{0,3}^{3,0}\left(0,\frac{1}{2},1\,\middle|\,\frac{\tilde{\Xi}_{\mathrm{I}}^2\tilde{\Xi}_{\mathrm{II}}}{4}\left(1+\frac{\Gamma\left(U+\frac{1}{2}\right)}{\Gamma(U)}\sqrt{\pi zp_0V}\right)^2\right)$$

$$- \frac{\tilde{\Xi}_{\mathrm{I}}\sqrt{\tilde{\Xi}_{\mathrm{II}}}}{2\sqrt{\pi}}\mathcal{G}_{0,3}^{3,0}\left(-\tfrac{1}{2},0,\tfrac{1}{2} \middle| \frac{\tilde{\Xi}_{\mathrm{I}}^2\tilde{\Xi}_{\mathrm{II}}}{4}\left(1+\frac{\Gamma\left(U+\frac{1}{2}\right)}{\Gamma(U)}\sqrt{\pi z p_0 V}\right)^2\right) \quad \text{(C.9)}$$

where $\tilde{\Xi}_{\mathrm{I}} = \frac{\pi\lambda}{\sqrt{p_0}}$ and $\tilde{\Xi}_{\mathrm{II}} = \frac{I_{\mathrm{SI}}}{\Omega}$. For the special cases without compensation and limit on the SI, we respectively obtain

$$\mathcal{M}_{\mathcal{I}}^{(\mathscr{E}\to 0,\mathscr{M}\to+\infty,p_0\to+\infty,K\to 0,\beta\to 4,\psi\to 1)}(z) = \frac{1}{\sqrt{\pi}}\mathcal{G}_{0,3}^{3,0}\left(0,\tfrac{1}{2},1 \middle| \frac{\pi^3\lambda^2 z V\tilde{\Xi}_{\mathrm{II}}}{4}\left(\frac{\Gamma\left(U+\frac{1}{2}\right)}{\Gamma(U)}\right)^2\right) \quad \text{(C.10)}$$

and

$$\mathcal{M}_{\mathcal{I}}^{(\mathscr{E}\to 0,\mathscr{M}\to+\infty,I_{\mathrm{SI}}\to+\infty,K\to 0,\beta\to 4,\psi\to 1)}(z) = \frac{1}{1+\frac{\Gamma\left(U+\frac{1}{2}\right)}{\Gamma(U)}\sqrt{\pi z p_0 V}}. \quad \text{(C.11)}$$

■

APPENDIX D

The DL and UL SE expressions respectively provided in (21) and (22) can be obtained directly through applying the m.g.f.-based approach in [37] to a stochastic geometry-based setting.

Consider the cases where the DL and UL SEs are respectively simplified to

$$\mathcal{S}_{d,f}^{(N^t=1,N^r=1,\mathcal{U}=1,K=0,\beta=4)} = \log_2(e)\int_0^{+\infty}\int_0^{+\infty}\int_0^{+\infty}\frac{2\pi\lambda^{(b)} r p^{(b)}}{(1+zp\Omega)\left(r^4+zp^{(b)}\right)} \exp\left(-\pi\lambda^{(b)}\left(\frac{\pi}{2}\sqrt{zp}+\sqrt{zp^{(b)}}\arctan\left(\frac{\sqrt{zp^{(b)}}}{r^2}\right)+r^2\right)\right)\mathcal{P}_{p_{x_k^l}^{(u)}}\,\mathrm{d}z\,\mathrm{d}r\,\mathrm{d}p \quad \text{(D.1)}$$

and

$$\mathcal{S}_{u,f}^{(N^t=1,N^r=1,\mathcal{U}=1,K=0,\beta=4)} = \log_2(e)\int_0^{+\infty}\int_0^{+\infty}\int_0^{+\infty}\frac{2\pi\lambda^{(b)} r p}{1+zp^{(b)}\Omega)\left(r^4+zp\right)} \exp\left(-\pi\lambda^{(b)}\left(\frac{\pi}{2}\sqrt{zp^{(b)}}+\sqrt{zp}\arctan\left(\frac{\sqrt{zp}}{r^2}\right)+r^2\right)\right)\mathcal{P}_{p_{x_k^l}^{(u)}}\,\mathrm{d}z\,\mathrm{d}r\,\mathrm{d}p. \quad \text{(D.2)}$$

Utilizing, in the order given, substitution with $\frac{z}{p^{(b)}} \to u^4$, conversion from Cartesian to polar coordinates with $u \to \mathscr{R}\sin(\mathscr{T})$ and $r \to \mathscr{R}\cos(\mathscr{T})$ (with Jacobian $\mathscr{R}$), the integral identity

$$\int_0^{+\infty}\frac{\mathscr{R}}{1+\mathscr{R}^4}\exp\left(-\mathscr{R}^2\right)\,\mathrm{d}\mathscr{R} = \frac{1}{2}\left(\sin(1)\,\mathscr{C}(1)+\left(\frac{\pi}{2}-\cos(1)\,\mathscr{S}(1)\right)\right), \quad \text{(D.3)}$$

and substitution with $\mathscr{T} \to \arctan\sqrt{s}$, we can arrive at (37). The same process can be applied in the case of complete SI removal but with the reduced integral identity (B.1) to obtain (38). Finally, we can respectively arrive at (39)-(40) using

$$\int_0^{+\infty}\frac{1}{p\left(p+\sqrt{p}\right)}\exp\left(-\frac{1}{p}\right)\,\mathrm{d}p = \sqrt{\pi}+\frac{1}{e}\mathrm{Ei}(1)-\frac{\pi}{e}\mathrm{erfi}(1) \quad \text{(D.4)}$$

and at (41)-(42) using

$$\int_0^{+\infty}\frac{1}{p+\sqrt{p}}\exp\left(-\sqrt{p}\right)\,dp = -2\exp(1)\mathrm{Ei}(-1). \quad \text{(D.5)}$$

■

APPENDIX E

By computing the special case of $2\left(\mathcal{S}_{d,f}+\mathcal{S}_{u,f}\right)$ and $\left(\mathcal{S}_{d,h}+\mathcal{S}_{u,h}\right)$ using the approach in Appendix D, we can readily obtain (43) and (44), respectively.

Utilizing the tight approximation (where $s \geq 0$)

$$\arctan(s) = \arcsin\left(\sqrt{\frac{s^2}{1+s^2}}\right) \geq \frac{s}{1+s}, \quad \text{(E.1)}$$

the integral identity (where $\alpha > \frac{1}{4}$)

$$\int_0^{\infty}\frac{1+s}{(1+s^2)\left(\alpha s^2+s+1\right)}\,\mathrm{d}s = \frac{1}{\sqrt{4\alpha-1}\left(\alpha^2-2\alpha+2\right)}\left(\pi\left(\alpha^2-\frac{\alpha}{2}\left(\sqrt{4\alpha-1}+3\right)+\sqrt{4\alpha-1}\right)\right.$$

$$+\frac{\alpha}{2}\sqrt{4\alpha-1}\log(\alpha)-\alpha(2\alpha-3)\operatorname{arccot}\left(\sqrt{4\alpha-1}\right)\Bigg), \quad \text{(E.2)}$$

and basic algebraic manipulation, we derive (45) and (46). ■

APPENDIX F

We proceed by defining the super-level set of $\frac{\mathbb{S}_f}{\mathbb{S}_h}$ in x as

$$\mathcal{L}=\left\{x\leq\Big|\frac{\mathbb{S}_f}{\mathbb{S}_h}\geq\mathscr{K}\right\}. \quad \text{(F.1)}$$

For the case in which $\mathscr{K}<0$, the total SE gain of FD over HD is always positive, hence, there are no points on the counter, $\left(\frac{\mathbb{S}_f}{\mathbb{S}_h}\right)^*=\mathscr{K}$. On the other hand, for $\mathscr{K}>0$, we can write

$$\frac{\mathbb{S}_f}{\mathbb{S}_h}=\frac{2\left(\mathcal{S}_{d,f}+\mathcal{S}_{u,f}\right)}{\mathcal{S}_{d,h}+\mathcal{S}_{u,h}}=\frac{\Psi\left(\frac{8}{\pi\left(1+\sqrt{x}\right)}-1\right)+\Psi\left(\frac{8}{\pi\left(1+\frac{1}{\sqrt{x}}\right)}-1\right)}{\Psi\left(\frac{8}{\pi}-1\right)} \quad \text{(F.2)}$$

with

$$\mathcal{L}\equiv\Psi\left(\frac{8}{\pi}-1\right)\mathscr{K}-\left(\Psi\left(\frac{8}{\pi\left(1+\sqrt{x}\right)}-1\right)+\Psi\left(\frac{8}{\pi\left(1+\frac{1}{\sqrt{x}}\right)}-1\right)\right)\leq 0. \quad \text{(F.3)}$$

The joint HD DL/UL SE in the above is affine in x. It can be shown that the second derivative of the FD mode SE function, $\frac{\mathrm{d}^2}{\mathrm{d}x^2}\left(2\left(\mathbb{S}_{d,f}+\mathbb{S}_{d,f}\right)\right)$, is always positive for $0<x<1$, always negative for $x>1$, and zero for $x=1$. Furthermore, $\mathcal{L}$ is convex in x. Hence, the objective function in (49) is strictly quasi-concave, with the maximum point occurring at $x=1$. ■